ESCOLA SUPERIOR DE SAÚDE
POLITÉCNICO DO PORTO

P.PORTO

M

MESTRADO
BIOQUÍMICA EM SAÚDE

Betulinic Acid properties in the invasive profile of glioblastoma

António José Silva Ferreira de Sousa

09/**2024**

ESCOLA
SUPERIOR
DE SAÚDE

Center for Translational Health
and Medical Biotechnology Research

Betulinic Acid properties in the invasive profile of glioblastoma

Author

António José Silva Ferreira de Sousa

Supervisors

Prof. Doutora Sílvia Fernandes, TBIO/RISE-Health, ESS-IPP

Prof. Doutor Ricardo Ferraz, TBIO/RISE-Health, ESS-IPP, LAQV-REQUIMTE

Project presented to fulfill the requirements necessary to obtain the degree of Master in **Biochemistry in Health – Applied Biochemistry** branch from the Escola Superior de Saúde of Instituto Politécnico do Porto.

Acknowledgements

First, I would like to thank my supervisors, Prof. Doutora Sílvia Fernandes and Prof. Doutor Ricardo Ferraz, for all their helpful contributions, availability and concern during the realization of this project.

To the Center for Translational Health and Medical Biotechnology Research (TBIO) and its members, I would like to give thanks for the opportunity to conduct this project, as well as for all the help and guidance received.

I would also like to mention all the professors and colleagues that were a part of this journey, as they enriched my knowledge and gifted me unforgettable memories.

Lastly, I want to thank my friends and family, for all the support and helping me be closer to my best version.

Abstract

Glioblastoma is the most frequent and most malignant primary brain neoplasia. The standard therapy, based on surgical resection, followed by radiation therapy and temozolomide, has not been effective. The complex system of signaling pathways and interactions with the extracellular matrix and host cells is at the root of the invasive phenotype of glioblastoma. For this reason, unveiling novel compounds and new therapeutic approaches against this cancer is of utmost importance. Betulinic acid has previously demonstrated selective antitumor activity in several cancer cell types as well as beneficial effects on neurological disorders, showing great potential to be used for glioblastoma treatment strategies.

The main objective of this work is to evaluate the effects of betulinic acid on the invasive profile of glioblastoma. Thus, A172 and U251 glioblastoma cell lines were treated with previously selected doses of betulinic acid and the effect on invasion and migration of the cells was evaluated through the transwell invasion assay and wound healing assay. Moreover, mRNA levels of different keyplayers were quantified using qPCR methodology.

The results showed that betulinic acid can counteract the migration pattern of glioblastoma cell lines, in all timepoints studied, particularly for the 2.5 μM dose. Alterations found on mRNA levels of some genes assessed in the present study seem to show that EGFR-STAT3 pathway blockade could be involved in the molecular action of BA. These are important findings regarding the molecular mechanisms involved in BA action, although further studies are needed.

The anti-invasive effects of betulinic acid, together with its ability to cross the blood-brain barrier and other anti-tumor properties, is a promising sign that this compound could constitute a novel therapeutic approach with better clinical outcomes.

Keywords: Glioblastoma; Betulinic acid; Migration; Invasion

Resumo

O glioblastoma é a neoplasia primária cerebral maligna mais frequente e mais agressiva. A terapia convencional, que consiste na resseção cirúrgica seguida de terapia de radiação e tomozolomida, não tem sido eficaz. O sistema complexo de vias de sinalização e interações com a matriz extracelular e células hospedeiras está na base do fenótipo invasivo do glioblastoma. Por esta razão, descobrir novos compostos e novas abordagens terapêuticas contra este cancro é de grande importância. O ácido betulínico demonstrou previamente atividade anti-tumoral seletiva em vários tipos de células tumorais, assim como efeitos benéficos em doenças neurológicas, mostrando grande potencial para ser usado em estratégias terapêuticas contra o glioblastoma.

O principal objetivo deste trabalho é avaliar os efeitos do ácido betulínico no perfil invasivo do glioblastoma. Assim, as linhas celulares de glioblastoma A172 e U251 foram tratadas com doses de ácido betulínico previamente selecionadas e o efeito na invasão e migração das células foi avaliado através do ensaio de invasão do *transwell* e do ensaio de *wound healing*. Além disso, os níveis de *mRNA* de diferentes genes-chave foram quantificados usando a metodologia *qPCR*.

Os resultados mostraram que o ácido betulínico consegue contrariar o padrão de migração de linhas celulares de glioblastoma, em todos os tempos de medição estudados, em particular na dose 2.5 μM. As alterações encontradas nos níveis de mRNA de alguns genes avaliados no presente estudo parecem mostrar que o bloqueio da via EGFR-STAT3 está na base da ação molecular do BA. Estes são achados importantes no que diz respeito aos mecanismos moleculares envolvidos na ação do BA, embora sejam necessários mais estudos.

Os efeitos anti-invasivos do ácido betulínico, juntamente com a sua capacidade de atravessar a barreira hematoencefálica e outras propriedades anti-tumorais, indicam que este composto pode constituir uma nova abordagem terapêutica com melhores resultados clínicos.

Palavras-chave: Glioblastoma; Ácido betulínico; Migração; Invasão

Index

Figure index

Abbreviations

ABCB1 – ATP Binding Cassette Subfamily B Member 1

ADAM – A Disintegrin and Metalloprotease

ADAMT – A Disintegrin and Metalloproteinase with Thrombospondin Motifs

AKT – AKT Serine/Threonine Kinase 1

BBB – Blood-Brain-Barrier

BCL-xL – B-cell Lymphoma-Extra Large

BDNF – Brain-derived Neurotrophic Factor

Camp – Cyclic Adenosine Monophosphate

CCND1 – Cyclin D1

CDK4 – Cyclin-dependent kinase 4

cGMP – Cyclic Guanosine Monophosphate

c-Myc – Cellular Myelocytomatosis

CNS – Central Nervous System

CSS – Cancer Stem Cell

CTLA-A – Cytotoxic T-lymphocyte Associated Protein

DMEM – Dulbecco's Modified Eagle Medium

DMSO – Dimethyl Sulfoxide

DNA – Deoxyribonucleic Acid

ECM – Extracellular Matrix

EDTA – Ethylenediamine Tetraacetic Acid

EGFR – Epidermal Growth Factor Receptor

EMT – Epithelial–Mesenchymal Transition

ERK – Extracellular Signal-Regulated Kinase

FAS-L – Fas Lingand

FBS – Fetal Bovine Serum

FSCN – Fascin

GB – Glioblastoma

GSC – Glioblastoma Stem Cell

Hh – Hedgehog

HIF-1α – Hypoxia Inducible Factor 1 Subunit Alpha

HSP – Heat Shock Protein

IC50 – Half Maximal Inhibitory Concentration

IDH1 – Isocitrate Dehydrogenase 1

IL – Interleukin

ILK – Integrin-Linked Kinase

JAK – Janus Kinase

LTP – Long-Term Potentiation

MAPK – Mitogen-Activated Protein Kinase

MDM2 – Mouse Double Minute 2

MGMT – O6-methylguanine-DNA Methyltransferase

miRNA – Micro RNA

MMP – Matrix Metalloproteinase

mRNA – Messenger RNA

NCAM – Neural Cell Adhesion Molecule

NF-Kb – Nuclear Factor Kappa B

NKC – Natural Killer Cell

PBS – Phosphate-Buffered Saline

PCR – Polymerase Chain Reaction

PD-1 – Death Protein 1

PI3K – Phosphatidylinositol 3-Kinase

qPCR – Quantitative PCR

RNA – Ribonucleic Acid

ROCK – Rho-Associated Protein Kinase

ROS – Reactive Oxygen Species

RT-PCR – Reverse Transcription PCR

SEM – Standard Error of the Mean

STAT3 – Signal Transducer and Activator of Transcription 3

TGF-β – Transforming Growth Factor Beta

TME – Tumor Microenvironment

TP53 – Tumor Protein 53

uPA – Urokinase-Type Plasminogen Activator

VEGF – Vascular Endothelial Growth Factor

WHO – World Health Organization

1. Introduction

1.1. Glioblastoma

Gliobastoma (GB) is a subtype of glioma that is particularly malignant, originating from malignant transformation of astrocytic glial cells (1). GB tumors are highly heterogeneous, being composed of diversified tumor cells and other tumor associated cells. Considering the specificity of each cell population and extracellular space, the interaction with their close microenvironment is essential to tumor development (2). The incidence of primary malignant brain tumors is approximately 7 per 100 000 individuals, around 49% of malignant primary brain tumors being GBs and 30% being diffusely infiltrating lower-grade gliomas. (3). There is geographical variation, with the incidence rate in developed countries being higher in comparison with developing countries, in general. Other factors also play a role as the incidence rate for gliomas in Japan is less than half in comparison with Northern Europe or the United States (4). The international standard for the nomenclature and diagnosis of gliomas is the World Health Organization (WHO) classification, in which GB is calssified as a grade-IV cancer (5).

The standardized treatment currently in place involves surgery for gross total resection, followed by a combination of radiation therapy and chemotherapy (with temozolomide). This treatment, however, has shown to be ineffective as mortality and recurrence remain high. The median overall survival since diagnosis is 14-15 months and the median recurrence time is approximately 6 months (6–8). Some causes behind the strong probability of recurrence include: incomplete resection, aided by the highly infiltrative nature of GB; high degree of genetic heterogeneity and GB stem cells (GSC) that can yield more aggressive recurrent tumors that are radioresistant and chemoresistant (9). There is currently no evidence that therapeutic approaches after recurrence have effects on survival, therefore there is no standardized treatment approach.

There are several complications that therarpies against malignant GB must overcome, the initial is the blood-brain barrier (BBB), comprised of endothelial cells interconnected by tight junctions (claudins, occludins, and junctional adhesion molecules) (10). The BBB permits only small (<500 Da and <400 nm) and lipophilic molecules to passively diffuse across, making it difficult for many therapeutic compounds to cross the barrier (11). Some pharmaceuticals may cross the BBB but in negligible amounts unable to generate the desired therapeutic effects.

Another difficulty for effective treatments in GB is tumoral heterogeneity, which includes a vast array of celular, molecular, genetic, spatial and temporal diversity that prevents the usage of any single universal therapeutic approach.

Moreover, the tumor microenvironment (TME) of GB, consisting of different types of cells in interaction with the extracellular matrix, cytokines and other growth factors in combination with hypoxia, acidosis and immunossupression, is able to promote treatment resistance and tumor cell proliferation. Hypoxia, resulting mainly from an increase in GB cell proliferation contributes to chemoresistance in several ways: regulation of CSSs (Cancer Stem Cells), enhancing their maintenance and chemoresistance; promoting resistance to pharmaceuticals that target highly proliferative cancer cells; confering radioresistance by reducing oxygen free radical formation; inhibiting pro-apoptotic pathways and stimulating antiapoptotic proteins; promoting angiogenesis, invasion, metastasis and genomic instability; inducing the recruitment of immune cells that support and amplify tumor vasculature expansion (12–16). Another TME feature that plays a role in treatment resistance is acidosis. Acidosis, that results from an increase in conversion of glucose to lactate associated with highly proliferative cells, contributes to tumor resistance by: promoting cell motility and migration; supporting the phenotype and resistance of CSS's; promoting angiogenesis; affecting the uptake and efficacy of different drugs; neutralizing reactive oxygen species (ROS) formation associated with radiotherapy; enhancing the pump activity of P-gp; promoting low proliferative rate of GB cells; playing a role in immunosuppression affecting Tcells, NKCs (Natural Killer Cells) , monocytes and CD8+ T cells (17–22).

The immunossuppressive microenvironment of GB is another factor that contributes to treatment failure, and is even worsened by some aggressive treatments like chemotherapy and radiation (23). This microenvironment is acquired by increased levels of factors that weaken the immune system (signal transducer and activator of transcription 3 (STAT3), death protein 1 (PD-1), Fas-Ligand (FAS-L)), expressed by cancer cells, TGF-β (Transforming Growth Factor Beta) and IL-1 secreted by microglia cells that promote local and systemic immunosuppression, upregulation of immune chechpoint molecules like IL-10, cytotoxic T-lymphocyte associated protein (CTLA-A) and immunosuppression by Treg and myeloid cells that have an immunosuppressive and tumor-promoting effect. Cytotoxic T lymphocytes, NKCs and tumor associated macrophages are also involved in the immunosuppression

process. Immunotherapy approaches like vaccine therapies are being studied currently, having the advantage of bypassing the obstacle of the BBB (24–29).

GB can also develop resistance to therapeutic agents through genetic aspects such as the absence of O(6)-methylguanine-DNA methyltransferase (MGMT) promoter methylation, which is reported in about 30-60% of patients with GB, and activates the mismatch repair (MMR) system pathways of cycle arrest and cell death. Defects in the MMR system are associated with treatment resistance. MicroRNAs (miRNAs), that have a fundamental role in tumor progression and invasion, also play a role in chemoresistance being involved in proliferation, cell death, invasion and drug sensitivity. MiRNAs are implicated in the expression of drug transporter genes or modulation of ABCB1 (ATP binding cassette subfamily B member 1)/P-gp-mediated multidrug resistance and are involved in cell-cell communication in pathological processes through their release into exosomes (30–35).

Multiple cytogenetic, chromosomal, and genetic alterations have been identified in GB, with distinct expression of antigens and some biomarkers that may alter therapeutic potential of this aggressive cancer. Intensive molecular analyses have revealed a variety of deregulated genetic pathways involved in DNA damage and repair, apoptosis, cell migration, angiogenesis, and the cell cycle. Some of the most commonly found genetic anomalies in patients with GB include: loss of heterozigoty on 10q (50-70%); EGFR (Epidermal Growth Factor Receptor) amplification (40-60%); P16ink4a deletion (31%); TP53 (Tumor Protein 53) mutation (50-60%); PTEN mutation (60%); MDM2 (Mouse Double Minute 2) polymorphism(40-60%); MGMT hypermethylation (50-60%); IDH1 (Isocitrate Dehydrogenase 1) mutation (40-60%); CDK4 (Cyclin-Dependent Kinase 4) mutation (20-30%); PDGFRA amplification (20-30%) (36).

Until now, few molecular biomarkers have been discovered. These include methylation of the MGMT promoter, IDH1 mutation, mutations in the promoter region of the telomerase reverse transcriptase gene, and amplification and/or overexpression of EGFR. These markers have shown potential to predict the survival outcomes and treatment response in GB patients (37).

Currently, the only confirmed risk factors for GB are radiation and certain genetic syndromes (Turcot syndrome, Neurofibromatosis type-1, Li-Fraumeni syndrome, Lynch syndrome) (38).

Despite growing understanding of the various mechanisms behind treatment failure, the standard therapy has not changed over the last decades, signifying a great impass and need for novel therapies.

1.2. Glioblastoma invasive profile

GB is a highly invasive tumor, invading the surrounding healthy tissue, but does not commonly migrate to organs outside the brain. GB cells are able to infiltrate through space around blood vessels or between neurons and glia (39). Although there is a considerable amount of information about the clinical and biological behaviour of gliomas, the high complexity of the invasion mechanisms remains a major challenge in clinical neuro-oncology (40).

The invasion process can occur through single-cell movement, amoeboid or mesenchymal, or through collective cell movement. Single cell movement consists of individual cells invading surrounding tissue (41). While mesenchymal migration requires moderate levels of Rho-associated protein kinase (ROCK) to contract the cell rear and retract protrusions, fast amoeboid migration relies on hyper-activation of ROCK-driven actomyosin contractility (42). A stufy showed that Integrin-linked kinase (ILK) promoted GB cell invasion through activation of ROCK1 and FSCN10 (Fascin-10) in vitro (43). On the other hand, collective migration involves the cooperative transport of whole groups of cells and is the predominant type of migration in GB (41). The collective movement is based on interactions of cells with other cells and the extracellular matrix (ECM). In these interactions, leader cells are sensitive to mechanical and chemical signals and exert influence in the motility of their follower cells (44).

The ECM has the function of providing structural and biochemical support to surrounding cells, consequently, also plays a key role in regulating migration and invasion (45). GB cells are able to modify ECM components, being capable of remodeling and degrading the matrix by matrix metalloproteinases (MMPs) released into the extracellular space. MMP-2 and MMP-9 are the most highly expressed MMPs in GB tissue, and they have been linked to a poor patient prognosis (46). MMPs break down cadherins, proteins that mediate cell-cell adhesion, thereby contributing to invasion (47). Although E-cadherin is a tumor suppressor protein, its expression in GB may indicate epithelial differentiation and is associated with proliferation and migration (48). Cathepsin, uPA (Urokinase-type Plasminogen Activator) and ADAMs/ADAMTs (A Disintegrin and Metalloproteinase/A Disintegrin and Metalloproteinase

with Thrombospondin Type 1 Motifs) demonstrate proteolytic activity and desintegrate components in the ECM allowing GB cells to invade (49–51). Molecules like NCAM (Neural Cell Adhesion Molecule) that mediate adhesion and migration, lower the production of MMPs and hinder invasion, are underexpressed in GB (52). Integrins, transmembrane receptors, are also involved in invasion by binding to extracelullar ligands and triggering signaling pathways that activate the motility mechanism (53,54).

The Wnt signaling pathway is involved in GB invasiveness, with the activation of the canonical Wnt/β-catenin pathway contributing to the stemness and mobility of GSCs through zinc finger E-box-binding homeobox 1 (ZEB1) activation. A study showed that Integrin α5β1 expression is involved in the β-catenin pathway activation in GB, thus being connected to cell migration (55). Wnt5a is also overexpressed in GSCs, modulating invasion by regulating MMP-2 expression and being involved in activating cell invasion genes (56–58).

TGF-β signaling promotes GSCs stemness and invasion by: activating the SOX4-SOX2 pathway, indirectly activating the transcription of the STAT pathway; regulating integrins, MMPs, MMP inhibitors and cathepsin (59–62). The JAK (Janus Kinase)/STAT pathway itself is essential to GB proliferation and metastasis. Specifically, the STAT3 gene, which is highly expressed in GB tissue and stimulates carcinogenic factors, has shown to promote proliferation and metastasis of GB cells (63).

The Hh (Hedgehog) pathway also promotes CSCs invasion and angiogenesis, inducing the expression of Slug factor, Snail factor and the vascular endothelial growth factor (VEGF) (64,65) and

Heat Shock Proteins (HSP) also play a role in tumorigenesis, mediating cancer self-sufficiency in growth signals. Specifically, the HSP90 is able to fold receptors and downstream molecules, stabilize AKT(AKT Serine/Threonine Kinase 1), EGFR and other factors that are implicated in proliferation, invasion and migration pathways (66,67).

The continuous study of the cellular and chemical mechanisms behind GB's invasive profile is of paramount importance, being at the genesis of the development of new therapeutic approaches.

1.3. Betulinic acid

Betulinic acid (BA, 3-beta-hydroxy-lup20(29)-en-28-oic acid; $C_{30}H_{48}O_3$), a pentacyclic triterpene, is distributed in a variety of plants and can be obtained by separation, chemical synthesis and biotransformation (68) (Figure 1).

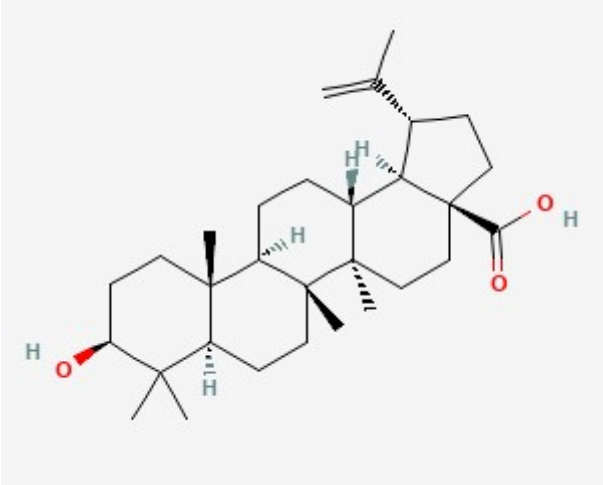

Figure 1: Chemical structure of Betulinic acid.

BA can be found as a natural product in *Menyanthes trifoliata*, *Paeonia emodi*, *Bowdichia virgilioides*, and other organisms (69). However, plant extraction of BA is not used for commercial purposes, as the reduced quantity of BA in plants results in an inefficient process with low extraction yields. Therefore, the production of BA for commercial purposes is through semisynthesis, via the oxidation of the primary hydroxyl group of the precursor botulin (70).

BA shows a wide spectrum of biological and pharmacological properties, such as anti-inflammatory, antibacterial, antiviral, antidiabetic, antimalarial, anti-HIV and antitumor effects (71–77).

BA has exhibited considerable potential as an antitumor agent, having shown anticancer activity in several neoplasms, such as: breast, bladder, ovarian, gallbladder, colorectal, gastric and lung (78–84). These effects have also been shown to be selective against tumor cells, although the specific mechanisms are still not understood.

Some mechanisms of action of BA against cancer have been elucidated more recently. In human cervical cancer cells, BA has been shown to induce apoptotic cell death by inhibiting phosphatidylinositol 3-kinase (PI3K)/AKT signaling and generating reactive oxygen species (85). BA has displayed the ability to regulate the JAK/STAT signaling pathway, which is a driver of carcinogenesis that stimulates factors like c-Myc (Cellular Myelocytomatosis), BCL-xL (B-Cell Lymphoma-Extra Large), MMPs, by dephosphotylation of STAT3 and inhibiting JAK (86–88). EGFR also plays a central role in cancer, and BA is capable of inhibiting this receptor

by preventing the cell signaling cascade that leads to invasion, migration and growth. In an in vitro study, BA was able to reduce the expression of MMP2 and MMP9 proteins, which are modulated by STAT3 (89). In another study, BA treated cancer cells showed an increase in E-cadherin expression, which is a marker of EMT (Epithelial-To-Mesenchymal Transition) inhibition (90). BA was also responsible for a decrease in expression of alpha-1 and alpha-2 integrins in human cancer cells, which are associated with invasion and migration (91,92).

BA has revealed the ability to decrease the mitochondrial outer membrane potential and inhibit antiapoptotic proteins while increasing the level of proapoptotic ones (72). Through inhibiting the expression and transcriptional activity of hypoxia-inducible factor-1α (HIF-1α) in hypoxic PC-3 prostate cancer cells, BA has shown anti-angiogenic activity (88). BA has also displayed the ability to inhibit the NF-kB (Nuclear Factor Kappa B) signaling pathway, a transcription factor frequently overexpressed in tumors (93). In another study, BA acted as an autophagy inducer through suppressing activation of the mitogen-activated protein kinase/extracellular signal-regulated kinase (MAPK/ERK) pathway in human hepatic stellate cells (94). Moreover, BA has shown the ability to control cancer proliferation through modulation of Sp transcription factors, inhibition of DNA topoisomerase, and inhibition of EMT (95).

Another characteristic of BA is that BA and its derivatives may act as sensitizers to optimize the clinical efficacy of cancer treatment, meaning they can be combined with already existing or novel treatments, in a potential future therapy (96).

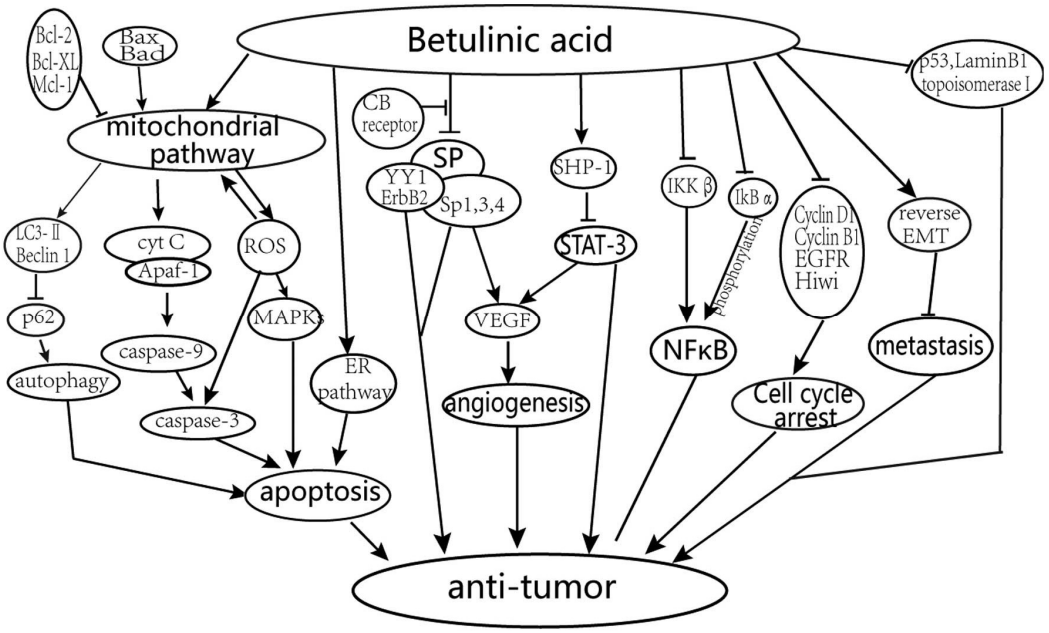

Figure 2: Representation of antitumor pharmacological effects of betulinic acid (92).

Regarding BA's effect in disorders of the central nervous system (CNS), some molecular insights have been found as well as important neuroprotective properties. In a study, BA showed it could improve the cognitive function, enhance antioxidant capacity, and inhibit the secretion of pro-inflammatory cytokines in the brain, playing a protective and preventive role against brain damage caused by the T-2 toxin (97). BA has shown the ability to scavenge free radicals and to remove oxidative agents in the brain tissue, being considered a possible therapeutic compound for motor and non-motor disorders in Parkinson's disease (98). BA pretreatment has shown to be able to prevent Alzheimer's disease induced neurobehavioral and LTP (Long-Term Potentiation) deficits in rats (99). In another study, BA was able to re-establish cerebral blood flow, restore behavioral parameters, restrain oxidative stress and inflammatory parameters, and improve cAMP (Cyclic Adenosine Monophosphate), cGMP (Cyclic Guanosine Monophosphate) and BDNF (Brain-Derived Neurotrophic Factor) levels. BA also demonstrated a neuroprotective effect in a dose-dependent manner (100).

Given all its antitumor and neuroprotective properties and its ability to cross the blood-brain-barrier, BA is a promising compound for GB treatment.

2. Objectives

This project aimed at evaluating the effects of BA on GB's invasive profile, using an in vitro approach. Using two different GB cancer cell lines, A172 and U251, the study aimed at characterizing mRNA (messenger RNA) expression levels of keyplayers having a role previously described in the literature. Moreover, migration and invasion profile of GB cell line was assessed, as well as the ability of different doses of BA to counteract the phenotype observed.

3. Methods

3.1. Cell lines

The cells studied were the A172 and U251 cell lines. The U251 cell line was derived from a malignant GB tumour by explant technique and the A172 cell line was isolated from the brain tissue of a 53-year-old with GB. Both cell lines have been used in GB research and were kindly provided by ICVS/3BS.

3.1.1. Cell thawing and cell freezing

Cell lines were cultured using the Dulbecco´s Modified Eagle Medium (DMEM, Gibco™, USA). Two stock solutions of DMEM with 10% and 20% fetal bovine serum (FBS, Alfagene, Portugal), and 1 % penicillin/streptomycin (Alfagene, Portugal), were prepared in aseptic conditions.

The cell lines stored at -80°C were suspended in DMEM media for centrifugation at 800 RPM for 5 minutes (Gyrozen, South Korea; 1248R). The supernatant was discarded, the pellet resuspended, and the cell lines were cultured in T75 culture flasks (Corning, USA) with DMEM media with 10% FBS. The cells were incubated at 37 °C and 5% CO^2 (PHCbi, MCO-170AICUVL-PA). The media was changed every two-three days until confluency was reached.

For cell freezing, aliquots containing the desired number of cells in suspension were added to cryogenic vials, as well as a solution of FBS with 10% DMSO (Dimethyl Sulfoxide), and stored at - 80°C.

3.1.2. Cell culture spliting

Cell splitting was performed when the cell flask reached confluency, meaning when most of the adhesive surface of the culture vessel was completely covered with cells. The old media was removed, cells were washed with phosphate-buffered saline (PBS) and incubated with 1 mL of trypsin-EDTA solution for approximately 5 minutes. Following incubation, 9 mL of media were added to the cells to stop the disaggregation effect of the trypsin. Afterwards, cells were centrifuged at 1200 RPM for 10 minutes. After discarding the old media and resuspending the cells in the appropriate media (DMEM with 10% FBS for cell culture and DMEM with 20% FBS for cell freezing), 20 μL of the cell suspension were mixed with 20 μL of trypan blue dye, and 10 μL transferred to a Neubauer Chamber for cell counting. When necessary, dilutions were made.

Finally, according to the determined final cell concentration, a defined volume of the suspension was added to the needed volume of media, transferred to the culture flask or assay plate, and incubated at 37 ºC and 5% CO2, or added to cryogenic vials for cell freezing.

3.1.3. Betulinic acid treatment

Stock solutions of DMEM media with different concentrations of BA (Sigma-Aldrich®, USA) (1 μM, 2.5 μM and 10 μM) were prepared in aseptic conditions in a laminar flow cabinet.

Due to the described instability of BA when dissolved in aqueous solutions, as DMEM media, the acid stock solutions were prepared using DMSO (101). However, the final BA stock solutions should not have a DMSO concentration higher than 1%, given its considerable cytotoxic effects (102,103).

In order to prepare the final DMEM/BA solutions, 1 mL of BA solutions, 100 times more concentrated than the final desired concentrations (100 μM, 250 μM and 1000 μM), were prepared by diluting the first two BA stock solutions with previously filtered DMSO. Then, 100 mL of each concentrated solution of BA were added to 9.9 mL DMEM media so that the final solutions had the desired BA concentration and 1% DMSO, thus preventing cell toxicity.

3.2. Gene expression analysis

3.2.1. RNA extraction

Cell culture splitting and cell counting was performed as previously described. Afterwards, a determined volume of the concentrated cell suspension was pipetted so that each 90mm petri dish had $5x10^5$ cells. After 24 hours of treatment with BA the media was removed, and cells were carefully washed with PBS and scrapped for nucleic acid extraction and analysis.

The extraction of RNA from the cultured cell lines, A172 and U251, was performed using the Lab-Aid 824s RNA Extraction Kit (Xiamen Zeesan Biotech Co., Ltd, China). The Lab-Aid 824s RNA Extraction Kit has advantages, such as: stable and reproductible extraction results; automated process, eliminating operator-dependent variability and the processing of large sample volumes, increasing the potential yield of RNA.

The procedure was comprised of 4 steps: lysis, binding, washing, elution, and is designed to ensure safe and reproducible handling of potentially infectious samples. The automated purification of nucleic acids based on magnetic particle technology combines the speed and efficiency of the instrument with the convenient handling of magnetic particles.

After UV disinfection, all the samples from the two cell lines were loaded in the equipment. Through the up-and-down movement of the magnetic rod sleeve, the samples were uniformly mixed, cracked, combined, washed, and finally eluted in the proper kit elution buffer. The extracted RNA samples were then stored at -20 °C before use.

3.2.2. RNA purity and concentration measurement

The concentration and purity measurement of the extracted RNA was performed using the UV/Vis spectrophotometer Thermoscientific Multiskan SkyHigh. This spectrophotometer is designed to be convenient and easy to use for virtually any photometric research application, especially DNA, RNA, and protein analysis, as well as turbidity measurements. In addition to common features, this spectrophotometer offers several advantages: rapid measurement of low sample volumes; flexibility; SkanIt software; Thermo Fisher Connect and Microsoft OneDrive.

To measure the concentration and the purity of the extracted RNA, 2μL of each sample were pipetted into the wells of the μDrop Duo Plate. Since the maximum absorbance of nucleic acids occurs at 260 nm, this wavelenght was selected, and the selected program initiated.

3.2.3. Quantitative PCR

To evaluate the effect of treatment with BA on the gene expression profile of the two cell lines, a two-step RT-PCR (reverse transcription PCR) was performed using the qTOWER^3 (Analytik Jena, Germany).

First, the extracted RNA was converted to cDNA with the Xpert cDNA Synthesis Kit. A mix was prepared containing: 5x Reaction Buffer; dNTP mix; Random Hexamer primer; Oligo(dT)$_{20}$ primer; Xpert Reverse Transcriptase and RNase free water. Then, a determined volume of purified RNA solution, containing 2 μg of nucleic acid of each BA treatment, was added to the mix to make up 20 μL. Next, the tubes containing mix and template were heated for 15 minutes at 50 °C. Finally, the reaction was stopped through inactivation of the reverse transcriptase by heating the tubes for 5 minutes at 85 °C and chilling on ice for 2 minutes.

Next, the cDNA synthesized was amplified using the SensiFAST™ SYBR® No-ROX Kit and specifically designed primers for the genes of interest. The primers for the tested genes (EGFR, ILK, MMP2, MMP9, E-Chaderin, Integrin $\alpha 5 \beta 1$, HSP90, AKT, STAT3) were designed with the Primer-Blast software and obtained from Stabvida. The primer sequences are in table 1.

Before the qPCR (quantitative PCR), a master mix containing 2x SensiFAST SYBR® No-ROX Mix, forward primer, reverse primer and water was prepared. Then, a determined volume of template was added to the mix to make up 20 μL, and the melting temperature of the primers was optimized: 58 °C for EGFR, MMP2, MMP9, HSP90, AKT and STAT3; 60 °C for ILK and Integrin $\alpha 5\beta 1$ and 62 °C for E-Cadherin.

Lastly, cDNA template from each BA treatment condition was added to the initial mix in the 96-well plate, the program with the adequate melting temperature for each primer was selected on the qTOWER^3, and the qPCR runs were initiated.

The results were obtained and analyzed using the comparative CT (ΔΔCT) method of relative quantitation, in which changes in gene expression in a given sample are compared to a housekeeping gene. The housekeeping gene used for comparative gene expression analysis was the GADPH gene. Experiments were done with 4 replicates of each treatment.

Table 1: Primer sequences used in qPCR.

Target gene	Forward primer (5'-3')	Reverse primer (5'-3')
AKT	CTCTTTCCAGACCCACGACC	ACAGGTGGAAGAACAGCTCG
E-Cadherin	GCTGGACCGAGAGAGTTTCC	CAAAATCCAAGCCCGTGGTG
EGFR	CCTGAGCTCTCTGAGTGCAA	TCTGGAGATGCTGGAGGGAG
GAPDH	AATGGGCAGCCGTTAGGAAA	GCCCAATACGACCAAATCAGAG
HSP90	CCAGAGTGCTGAATACCCG	TAACAGGTGCCCTGCTTCTC
ILK	CCCGAGTCCCGTCCTCA	TCGTTCTCCGTGTTGTCCAG
Integrin α5β1	TCGGGGGCTTCAACTTAGAC	CAGGAGCCGAGAGCCTTTG
MMP2	GGACTTAGACCGCTTGGCTT	GTGTTCAGGTATTGCATGTGCT
MMP9	GTACTCGACCTGTACCAGCG	TTCAGGGCGAGGACCATAGA
STAT3	AGCAGTTTCTTCAGAGCAGGT	AGGCGTGATTCTTCCCACAG

3.3. Wound healing assay

For the wound healing assay, U251 cells were cultured, and cell culture splitting and counting was performed as previously described. After determining the concentration of the cell suspension, a volume was calculated and pipetted so that each well in the 6-well plate had approximately 1x10^5 cells. Then, cells were cultured in DMEM media with 10% FBS and 1% P/S, until reaching around 80% confluency. Next, the old media was removed, the culture was carefully washed with PBS and a line was drawn with a pipette tip to create the "wound". Previously prepared BA solutions in DMEM media were added to the wells of the 6-well plate. In order to ensure analysis of cell migration and minimize the effect of cell proliferation, DMEM

media was not supplemented with FBS. Photographs were taken in specific places to record the initial stage of the wound, and the cells were incubated.

Afterwards, several photographs were taken at different timepoints (8h, 24h, 32h, 48h) in the same places of the photographs taken at timepoint 0h.

Then, using the image software ImageJ, the percentage of wound area covered by migrated cells at the different timepoints was measured. To the total area of the wound, the area occupied by migrated cells was subtracted, and the percentage of wound area covered was calculated (see the Results section). Each treatment concentration was applied in 4 wells, with measurements in two different wound sections, resulting in 8 replicates for each group.

3.4. Transwell invasion assay

For the transwell invasion assay, U251 cells were cultured and cell culture splitting was done as described above and cells were cultured in DMEM media with 10% FBS and 1% P/S, until reaching around 80% confluency. Afterwards, matrigel was thawed overnight at 4°C and the stock solution of matrigel was diluted with sterile water (1:1). Next, 70-80 μL of matrigel were added to the upper compartment of the insert and the 24-well plate was incubated for 45 minutes at 37 °C and 5% CO2.

Then, cell counting was performed as previously described and a defined volume of the cell suspension was added to the needed volume of media to prepare a final suspension with a concentration of $1x10^6$ cells/mL.

Afterwards, 100 μL of each cell suspension ($1x10^5$ cells) in DMEM media were pipetted onto the matrigel and incubated for 10 minutes at 37 °C and 5% CO2.

Then, 600 μL of DMEM supplemented with 10 % FBS were added to the well directly below the insert. The 24-plate well was incubated for 24 hours at 37 °C and 5% CO2.

For counting the adherent cells, the matrigel was removed from the transwell insert using a cotton tipped applicator to remove all non-migrated cells. The transwell insert containing media was placed into a well containing 1 mL of PBS to wash the membrane. Following that, the insert was placed in another well with 1 mL of methanol and incubated for 10-15 minutes at room temperature to fixate the migrated cells, and the transwell insert was allowed to dry.

Next, colorimetric staining was performed. The transwell insert was placed in a well with Giemsa dye and incubated for 3-5 minutes at room temperature. After that, the insert was removed and placed in another well containing PBS to remove the remaining dye, and the

membrane was allowed to dry. Then, 6-8 representative images of the insert's lower membrane were obtained using a microscope with a 10x or 20x objective, for each treatment condition. Lastly, the images were analyzed with ImageJ software and the percentage of insert membrane covered by adherent cells was calculated by subtracting the area covered by fixated cells to the total area of the image. Experiments were done with 4 replicates of each treatment concentration.

3.5. Statistical analysis

Statistical analysis of the results obtained were performed using the GraphPad Prism software (version 10.1.2, San Diego, USA). The results are expressed as mean ± SEM. To analyze the normality of the data, the Shapiro-Wilk test was used. According to the results, the ordinary one-way ANOVA, followed by Tukey's multiple comparisons test, or the Kruskal-Wallis test, followed by Dunn's multiple comparisons test, were used to determine the significance of the differences between data groups. A significance level (alpha) of 0.5 was used.

4. Results

4.1. Viability assays for BA dose determination

In a previous work done by the same research team, the IC50 (half-maximal inhibitory concentration value) values for each cell line were calculated. The IC50 of BA is a measure of the concentration at which this compound reduces cell viability by 50%. The selection of the optimal BA concentrations to use for minimizing the interference of cell death on the other assay's results was based on previously obtained cell viability results.

After 24 hours of treatment, BA showed an IC50 value of 41.90 μM and 228.4 μM for U251 and A172 cells, respectively. After 48 hours of treatment, BA showed an IC50 value of 39.02 μM and 40.77 μM for U251 and A172 cells, respectively. These results showed that BA affects GB U251 cell line's viability, and that the A172 cell line seems to be more resistant to the same BA doses in comparison with the U251 cell line, at 24h treatment, with a decrease of viability achieved only for 10 μM dose

Following assays were performed using BA concentration values equivalent to IC20 and IC30, meaning a cell viability inhibition rate not higher than 20-40%.

4.2. Gene expression through qPCR

4.2.1. A172 cell line

Figure 3 represents the relative fold change values ($2^{-\Delta\Delta Ct}$) of several genes of interest (AKT, EGFR, E-Cadherin, HSP90, ILK, Integrin- α 5 β 1, MMP9 and STAT3) obtained through qPCR following treatment of the A172 cell line with various concentrations of BA (10 μM, 2.5 μM and 1 μM).

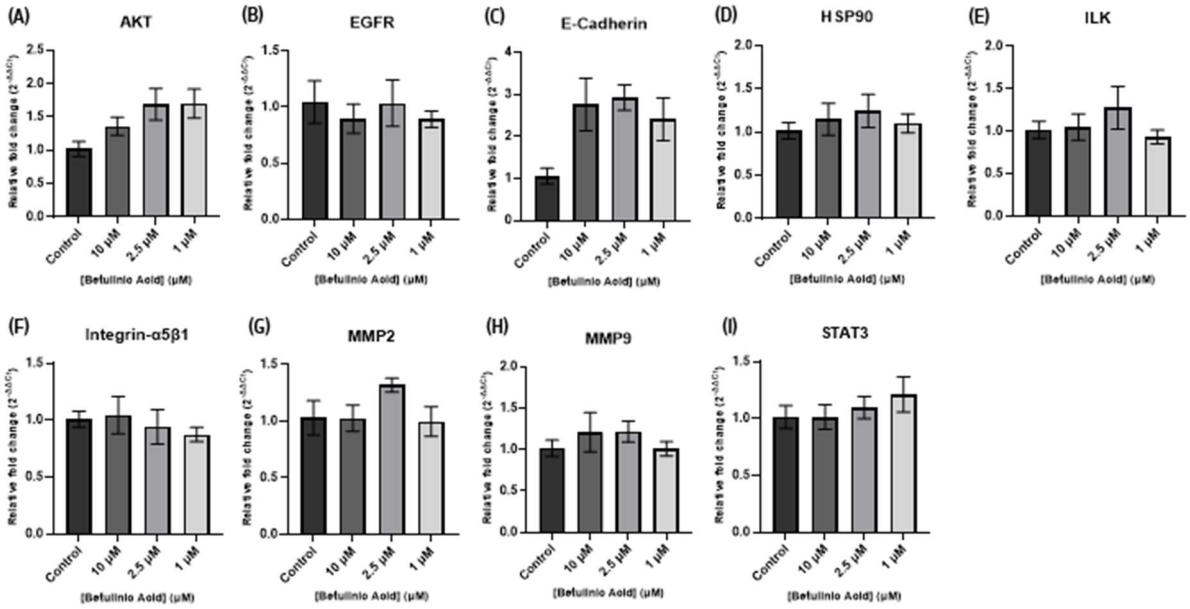

Figure 3: A172 cell line relative fold change ($2^{-\Delta\Delta Ct}$) at different treatment concentrations of BA for several genes: AKT (A), EGFR (B), E-Cadherin (C), HSP90 (D), ILK (E), Integrin-α5β1 (F), MMP2 (G), MMP9 (H) and STAT3 (I). Results are presented as Mean +/- SEM. *p<0.05, **p<0.01, ***p<0.001, ****p<0.0001.

For the AKT gene, the relative fold change values were 1.02 (SEM=0.11) for the control, 1.36 (SEM=0.14) for the 10 μM BA group, 1.69 (SEM=0.2363) for the 2.5 μM BA group and 1.70 (SEM=0.22) for the 1 μM BA group. There were no statistically significant differences observed between the different treatments.

The relative fold change values for the EGFR gene were 1.04 (SEM=0.19), 0.89 (SEM=0.13), 1.03 (SEM=0.20) and 0.8899 (SEM=0.07) for the control, 10 μM, 2.5 μM and 1 μM groups, respectively. No statistically significant differences between the treatments were detected.

The E-cadherin gene showed values of relative fold change of 1.05 (SEM=0.19) for the control group, 2.76 (SEM=0.62) for the 10 μM group, 2.92 (SEM=0.30) for the 2.5 μM group and 2.40 (SEM=0.51) for the 1 μM group. Although an important trend to increase E-cadherin expression after BA treatment, no statistically significant differences in fold change value between the treatments were found.

For the HSP90 gene, the relative fold change values for the control, 10 μM, 2.5 μM and 1 μM groups were 1.01 (SEM=0.09), 1.14 (SEM=0.18), 1.24 (SEM=0.19) and 1.09 (SEM=0.11), respectively. Statistical analysis revealed no statistically significant differences between treatments in this gene.

Next, the ILK gene showed values of relative fold change equivalent to 1.02 (SEM=0.10) for the control group, 1.05 (SEM=0.15) for the 10 μM group, 1.27 (SEM=0.25) for the 2.5 μM group and 0.93 (SEM=0.08) for the 1 μM group. Again, no statistically significant differences were identified between the different treatment concentrations.

The relative fold change values for the Integrin-α5β1 gene were 1.01 (SEM=0.07) for the control group, 1.04 (SEM=0.16) for the 10 μM group, 0.94 (SEM=0.15) for the 2.5 μM group and 0.87 (SEM=0.06) for the 1 μM group. No difference in fold change value between treatments was statistically significant.

For the MMP2 gene, the relative fold change values for the control, 10 μM, 2.5 μM and 1 μM groups were 1.03 (SEM=0.15), 1.03 (SEM=0.11), 1.32 (SEM=0.06) and 1.00 (SEM=0.13), respectively. No statistically significant differences between treatments were found after statistical analysis.

Next, MMP9s values of relative fold change were 1.01 (SEM=0.09), 1.21 (SEM=0.24), 1.21 (SEM=0.12) and 1.01 (SEM=0.08) for the control, 10 μM, 2.5 μM and 1 μM groups, respectively. No statistically significant differences were observed in this gene.

Lastly, the STAT3 gene presented values of relative fold change value of 1.01 (SEM=0.10) for the control group, 1.01 (SEM=0.11) for the 10 μM group, 1.09 (SEM=0.09) for the 2.5 μM group and 1.21 (SEM=0.15) for the 1 μM group, respectively. There were also no statistically significant differences observed between the different treatments.

Overall, using the A172 cell line, the study did not allow to find any significant changes after BA treatment of the cells.

4.2.2. U251 cell line

Figure 4 represents the relative fold change values ($2^{-\Delta\Delta Ct}$) of several genes of interest (AKT, EGFR, E-Cadherin, HSP90, ILK, Integrin-α5β1, MMP9 and STAT3) obtained through qPCR following treatment of the U251 cell line with various concentrations of BA (10 μM, 2.5 μM and 1 μM).

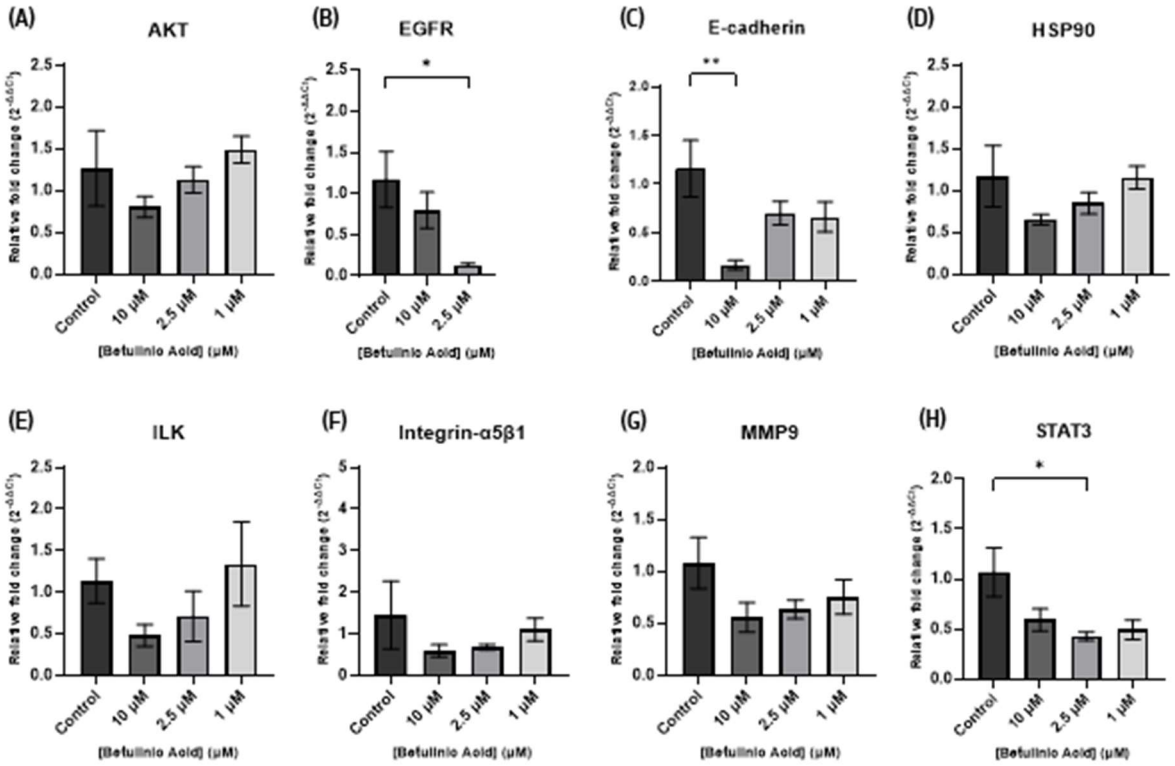

Figure 4: U251 cell line relative fold change ($2^{-\Delta\Delta Ct}$) at different treatment concentrations of BA for several genes: AKT (A), EGFR (B), E-Cadherin (C), HSP90 (D), ILK (E), Integrin-α5β1 (F), MMP9 (G) and STAT3 (H). Results are presented as Mean +/- SEM. *p<0.05, **p<0.01, ***p<0.001, ****p<0.0001.

For the AKT gene, the relative fold change values are 1.26 (SEM=0.45) for the control, 0.80 (SEM=0.12) for the 10 μM group, 1.12 (SEM=0.15) for the 2.5 μM group and 1.49 (SEM=0.16) for the 1 μM group. There were no statistically significant differences in fold change value between the treatments.

Regarding the EGFR gene, the values of relative fold change for the control, 10 μM and 2.5 μM groups are 1.17 (SEM=0.34), 0.79 (SEM=0.22) and 0.13 (SEM=0.02), respectively. In this assay there was a statistically significant difference between the control and the 2.5 μM group, revealing a decrease of 1.04 (p=0.0284) in fold change value. Due to a technical issue occurred, no results are available regarding 1 μM treated cells.

Next, for the E-cadherin gene, the fold change values are 1.16 (SEM=0.29) for the control, 0.16 (SEM=0.04) for the 10 μM group, 0.70 (SEM=0.12) for the 2.5 μM group and 0.66 (SEM=0.15) for the 1 μM group. There was a statistically significant difference between the control and 10 μM group equal to 1.00 (p=0.086) in relative fold change value.

For the HSP90 gene, the relative fold change values for the control, 10 μM, 2.5 μM and 1 μM groups were 1.17 (SEM=0.36), 0.65 (SEM=0.06), 0.85 (SEM=0.13) and 1.15 (SEM=0.13),

respectively. Statistical analysis revealed no statistically significant differences between the treatment groups.

The relative fold change values for the ILK gene were 1.13 (SEM=0.26) for the control group, 0.48 (SEM=0.13) for the 10 μM group, 0.71 (SEM=0.30) for the 2.5 μM group and 1.34 (SEM=0.50) for the 1 μM group. No difference in fold change value between the treatment groups was statistically significant.

For the Integrin-α5β1 gene, the fold change values were 1.45 (SEM=0.81), 0.59 (SEM=0.14), 0.68 (SEM=0.06) and 1.09 (SEM=0.27) for the control, 10 μM, 2.5 μM and 1 μM groups, respectively. No statistically significant differences between the treatments were detected after statistical analysis.

The fold change values for the MMP9 gene were 1.08 (SEM=0.24) for the control group, 0.56 (SEM=0.14) for the 10 μM group, 0.63 (SEM=0.09) for the 2.5 μM group and 0.75 (SEM=0.16) for the 1 μM group. There were no statistically significant differences in fold change value between the different treatments.

Lastly, the STAT3's relative fold change values for the control, 10 μM, 2.5 μM and 1 μM groups are 1.07 (SEM=0.24), 0.59 (SEM=0.11), 0.43 (SEM=0.04) and 0.49 (SEM=0.09), respectively. A statistically significant difference was observed between the control and 2.5 μM group, with the latter showing a reduction equivalent to 0.64 ($p=0.0367$) in fold change value.

4.3. Wound Healing Assay

Figure 5 shows some of the photographs taken in specific places of the wound, of the control, BA 1μM and BA 2.5μM treatments at 0h, 8h, 24h, 32h and 48h timepoints.

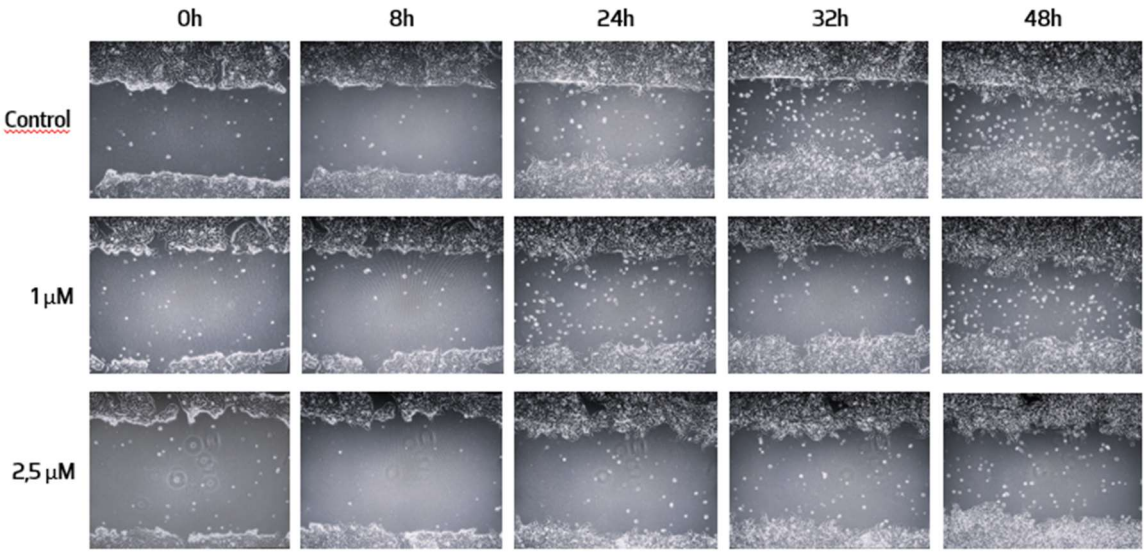

Figure 5: Representative photographs of the Wound Healing Assay of the control, BA 1 µM and BA 2.5 µM groups at 0h, 8h, 24h, 32h and 48h.

Figure 6 shows the percentage of wound area covered of all treatment concentrations (control, BA 1 µM and BA 2.5 µM) at the different timepoints (8h, 24h, 32h and 48h).

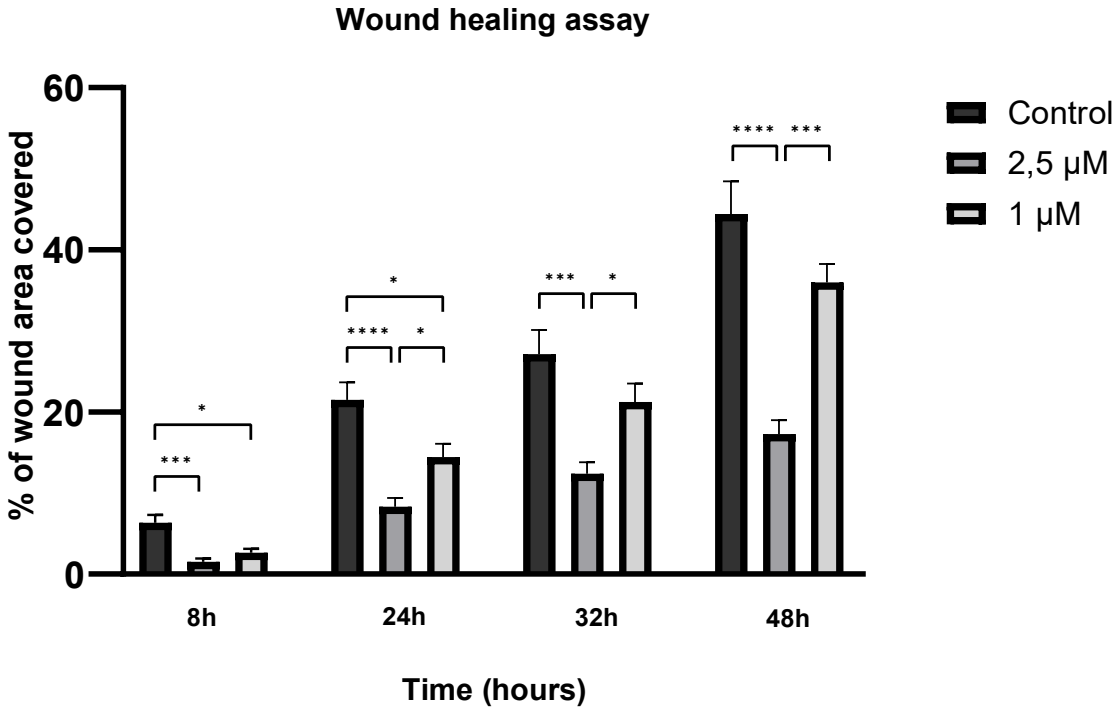

Figure 6: Percentage of wound area covered in different treatment groups (control, BA 2,5 µM and BA 1 µM) at different timepoints (8h, 24h, 32h, 48h). Results are presented as Mean +/- SEM. *p<0.05, **p<0.01, ***p<0.001, ****p<0.0001.

At 8 hours after BA treatment, the average percentage of wound area covered in the control group was 6.33% (SEM=0.95). The average percentages of wound area covered in the wells treated with 1 μM and 2.5 μM BA were 2.61% (SEM=0.52) and 1.49% (SEM=0.43), respectively. Statistically significant differences were observed between the control group and the group treated with 2.5 μM BA, in which migration was inhibited by 4.84% (p=0.0005).

In the 24-hour timepoint, the average percentages of wound area covered were 21.48% (SEM=2.16), 14.44% (SEM=1.61) and 8.31% (SEM=1.09) for the control, 1 μM and 2.5 μM BA groups, respectively. The biggest difference was observed between the control and the 2.5 μM group, showing a reduction of 13.17% (p<0.0001) in wound area coverage.

The average percentages of wound area coverage at 32 hours after treatment were 27.12% (SEM=2.99) for the control group, 21.21% (SEM=2.29) for the 1 μM group and 12.36% (SEM=1.41) for the 2.5 μM group. In this timepoint, the difference between the control group and the 1 μM group was not statistically significant. The biggest statistically significant difference was observed between the control and the 2.5 μM group, with the latter showing a reduction in wound area coverage of 14.76% (p=0.0006) in comparison with the control group.

In the last timepoint, 48h, the average percentages of wound area covered were 44.42% (SEM=4.03), 35.96% (SEM=2.28) and 17.27% (SEM=1.71) for the control, 1 μM and 2.5 μM groups, respectively. The difference between the control and 1 μM groups was not statistically significant. The most considerable difference was observed between the control group and the 2.5 μM group, with a reduction of 27.15% (p<0.0001) in cell migration.

The BA 1 μM treatment condition reduced cell migration in all timepoints in comparison with the control group, with statistically significant differences at 8h and 24h. This treatment condition reduced migration by 3.72% (8h), 7.04% (24h), 5.91% (32h) and 8.46%(48h).

The BA 2.5 μM treatment condition also reduced cell migration in comparison with the control group, with statistically significant differences in all timepoints. This treatment condition reduced cell migration by 4.84% (8h), 13.17% (24h), 14,76% (32h) and 27.15% (48h).

Overall, the results showed that cell culture plates treated with BA displayed less cell migration and less coverage of the wound in comparison with the control group in all timepoints.

Also, BA seems to have halted migration in a manner proportional to its concentration.

4.4. Transwell invasion assay

Figure 7 shows representative images of the Transwell Invasion Assay after treatment of U251 cells with different concentrations of BA.

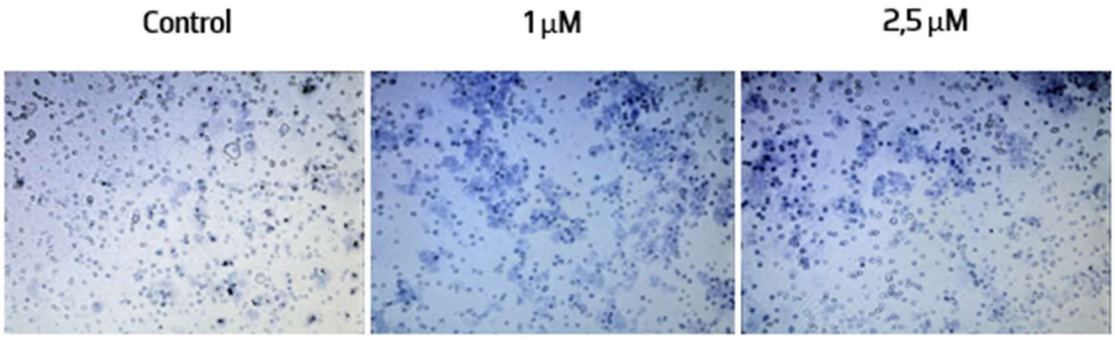

Figure 7: Representative photographs of U251 adherent cells on the insert membrane of the control, BA 1 μM and BA 2.5 μM treatment conditions.

Figure 8 represents the percentage of insert membrane covered with U251 cells after the Transwell Invasion Assay, for the control, BA 1 μM and BA 2.5 μM treatment conditions.

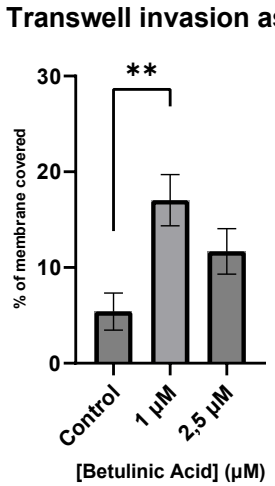

Figure 8: Percentage of insert membrane covered by adherent U251 cells after treatment with BA (control, BA 1 μM and BA 2.5 μM). Results are presented as Mean +/- SEM. *p<0.05, **p<0.01, ***p<0.001, ****p<0.0001.

Invasive cells on the lower surface of the insert membranes were stained and quantified. The average percentage of surface covered with invasive cells for the control, 1 μM and 2.5 μM groups was 5.40% (SEM=1.93), 17.03% (SEM=2.67) and 11.69% (SEM=2.38). Statistically significant differences were observed between the control and the 1 μM groups, with an increase in cell invasion in the 1 μM group equivalent to 11.63% (p=0.0085). The difference in cell invasion between the control and 2.5 μM group was not statistically significant. The effect of BA on invasion was ambiguous, being impossible to correlate BA treatment concentration and cell invasion.

5. Discussion

There is currently a great necessity for new therapeutic approaches for GB, the most common and malignant type of primary brain tumor, since the current approach is not as effective as desired. Due to BA antitumor activity in several neoplasms as well as the ability to cross the blood-brain-barrier, it is a promising compound for developing a novel therapy for GB treatment. The present study aimed at evaluating antitumor properties of BA, namely its effects on GB cell migration, invasion and gene expression of determined molecular targets using an in vitro model.

Based on previous results from the Metabonomics, Obesity & Related Disorders (MORD) research group, where the invasive profile of a GB cell line was altered with BA treatment, a screening through mRNA levels of the main molecular targets described in the literature was made. In the A172 cell line, although there were some differences in fold change value that may indicate BA's antitumor activity, there were no significant differences between treatment groups in what concerns the molecular pattern expression under analysis. These results may be explained by A172 cell line's distinctive behavior shown by previous viability studies, in which this cell line had a higher IC50 value at 24h than the U251 cell line, meaning more resistance to BA. Thus, further studies are necessary to better understand the mechanisms involved in the A172 cell line, as well as the respective effect of BA on its migration profile.

Regarding the evaluation of BA effects on the U251 cell line, important statistically significant differences were found on EGFR, E-Cadherin and STAT3 genes expression. EGFR is often overexpressed and/or hyper-activated in human malignant neoplasms, including GB, and therefore EGFR-directed therapeutic strategies are often utilized (104). In the present study, treatment of U251 cells with BA 2.5 μM reduced the expression of the EGFR gene by 1.04 in fold change in comparison with the control, indicating a potential anticancer activity of BA via EGFR in U251 cells. These results support the possibility that BA inhibited, directly or indirectly, the EGFR signaling pathway, involved in GB cell survival, proliferation and migration, corroborating other studies (105–107). Thus, EGFR mediated activation of signal transduction pathways like the PI3K/AKT/mTOR, RAS/MAPK, JAK/STAT may be inhibited by BA. The PI3K/AKT/mTOR pathway stimulates the expression of NF- kB, HIF-1α and VEGF, factors that play an important role in EMT, cell proliferation, invasion and cell death evasion (108). The RAS/MAPK pathway activation leads to the expression of the transcription factor activator protein, also playing a role in cell proliferation and invasion (109). Besides, the JAK/STAT3

pathway is associated with cell migration by promoting the expression of MMPs, HIF-1, c-Myc, BCL-xL and the VEGF (110). Moreover, EGFR was proven to influence the glutamine metabolism in glioma cells, important in hypoxic conditions (111).

The treatment with BA 2.5 μM also caused an evident reduction in the expression of STAT3 gene, equivalent to 0.64 in fold change, which indicates the potential suppression of the STAT3-mediated signaling pathway involved in GB carcinogenesis. The literature described that by reducing STAT3 expression and consequently the JAK/STAT pathway, BA suppresses CCND1 (cyclin D1), c-Myc, BCL-xL and MMP's, that are involved in cell cycle progression, invasion, migration and cell death evasion (45,86,112–114). The JAK/STAT3 pathway is therefore involved in GB cell migration, invasion and proliferation, by upregulating MMPs that degrade the ECM and facilitate migration. This pathway is also involved in the expression of focal spot kinase (FAK), which is implicated in cell cycle regulation, cell death evasion, EMT and TME remodeling (115). A study showed that miR-182-5p, induced by STAT3, promoted GB cell proliferation, migration and invasion (116). The STAT3 pathway can also be involved in tumorigenesis by interacting with HIF-1 and VEGF (117). Although STAT3 cannot directly regulate VEGF transcription, its activation via PI3K/AKT pathway is indispensable to the process (108). Another way STAT3 contributes to GB aggressiveness and invasiveness is through maintaining the pluripotency of GSCs (118), that play a role in invasion as previously described. The RTVP-1 overexpression, associated with STAT3 expression, facilitated GB cell invasion and growth (119). Other mechanisms of STAT3 driven tumorigenesis that may play a role in migration include conversion of aerobic respiration to glycolysis (120) and regulation of the intercellular adhesion molecule 1 (121).

In the present study, the STAT3 gene expression reduction observed with 2.5 μM BA dose is accompanied by a suppression of the cell migration analyzed through the wound healing assay. This reduction in migration could be explained by the suppression of the JAK/STAT3 signaling pathway, which is implicated in cell migration, as previously described. The STAT3 downregulation is likely involved in the reduced migration phenotype observed, meaning that BA probably interfered, directly or indirectly, in one or several pathways involving STAT3. These results corroborate other assays in which STAT3 inhibition resulted in reduced cell migration (122–125). Overall, the statistical differences in the EGFR and STAT3 genes assessed in the present study seem to corroborate that EGFR-STAT3 pathway blockade could

be involved in the molecular action of BA, as well as other antitumor therapeutic agents described in the literature (126–128).

The present study also revealed a significant reduction in fold change value for the E-cadherin gene, only in BA 10 μM-treated cells. Since the E-cadherin gene encodes a tumor suppressor protein, BA should cause an increase in its expression, however, this was not observed in the present work.

In a study by Sun et al, treatment with BA caused a reduction in cell migration in the wound healing assay, while at the same time causing an increase in E-cadherin expression (epithelial marker) and a decrease in vimentin expression (mesenchymal marker). The fact that in this study the expression of E-cadherin, an epithelial marker, was elevated, may be explained by BA-mediated suppression of the EMT transition (90). The downregulation of E-cadherin and upregulation of N-cadherin and other EMT markers is associated with higher tumor aggressiveness (129). However, this study did not quantify the transition of the different types of cadherin, so it is not possible to conclude about this molecular mechanism in our cancer cell model.

Another study showed that E-cadherin may play a "double agent" role in cancer, being a tumor suppressing protein that can also assist tumor cell survival and enhance invasive and metastatic potential (130). BA may have halted E-cadherin expression, directly or indirectly, through its antitumor properties. Also, based on a high cytotoxic effect, particularly observed in U251 cell line after BA 10 μM treatment, this reduced expression may be attributed to other processes, so caution is needed to conclude about this. Indeed, BA 2.5 μM and 1 μM did not significantly alter the mRNA levels expression of E-cadherin, although a trend is observed.

BA's effect on U251 cell line migration was studied via the Wound Healing Assay. This assay consists in a line drawn with a pipette on a confluent cell culture plate. Cells will then migrate to reoccupy the created wound, in a process that involves several pathways and can be influenced by several factors and external compounds. Thus, this methodology allows for testing the effects of different compounds on cell migration, in an inexpensive way without special equipment. It is also important that proliferation/viability assays are performed beforehand to assess the influence of the compounds' toxicity on cell migration. This technique can be done in association with other assays, in order to validate or corroborate results. Here, different BA concentration treatments, selected based on previous cell viability results were used to test BA's potential anti-migration effects.

The results showed that BA reduced cancer cell migration in all treatment concentrations and in all timepoints studied. There was a direct relation between the reduction in wound area covered and BA treatment concentration, with the biggest reductions in wound area covered corresponding to the highest concentrations of BA. BA 2.5 μM treated group showed the biggest reduction in migration, followed by the BA 1 μM treated group, when compared to the control group. Our results agree with results from other studies, where a reduction in migration was observed after treatment with BA (92,136–138).

These results seem to substantiate the qPCR results, in which the BA 2.5 μM reduced the expression of EGFR and STAT3, both involved in GB migration. Higher doses of BA resulted in less cancer cell migration to the wound, with the possible involvement of JAK/STAT pathway inhibition, resulting in reduced cell cycle progression, invasion, migration and cell death evasion, as previously observed (86). Moreover, STAT3 inhibition may also have hindered migration through other mechanisms mentioned above. Besides, BA may also have simultaneously inhibited the EGFR signaling cascade that is involved in GB cell migration, proliferation and apoptosis (104), as formerly described.

The inhibition of other pro-tumor pathways have been described and could also be involved in our cell model, such as the inhibition of NF-Kb signaling pathway, the regulation of TRAIL-mediated apoptosis, the inactivation of PI3K/AKT/mTOR signaling and/or the blockade of Sp1-mediated upregulation of VEGF (131–135).

Although the wound healing assays' results corroborate with the differences observed in the mRNA levels of EGFR and STAT3 genes, other statistically significant differences in other genes were expected, such as: ILK, MMPs, AKT, Integrin-$\alpha 5\beta 1$ or HSP90. Although a general trend is visible, where at least the lower concentrations of BA reduce the expression of genes involved in migration and invasion, there are no statistically significant differences. These results contradict the literature that supports the direct or indirect involvement of the expression of these genes in GB migration and invasion (43,47,55,67). Due to lack of time, the proteolytic activity of MMP2 and MMP9 proteins was not analyzed. Here, although no statistically significant differences in gene expression were observed, zymography could allow a better comprehension of BA's effects on migration and interaction with the ECM. In several studies, BA treatment of cells lines resulted in suppression of protein activity of MMP2 and MMP9 (136–138). Quantification of ILK protein, a promoter of invasion and migration

through activation of ROCK and FSCN, or of Integrin-α5β1, involved in the β-catenin pathway could also give important insights for better understanding BA antitumor mechanisms.

Lastly, to study BA's effects on GB invasion, the Transwell Invasion Assay was performed by treating U251 cells with different concentrations of BA. Unexpectedly, the results after the matrigel invasion assay showed an increased number of cells passing the matrigel, which is probably correlated with an increased invasion. Those results are not in agreement with qPCR and migration results obtained through the wound healing assay. Considering BA anti-invasiveness effects described in several articles (92,139,140), these results were not expected as BA seems to promote cell invasion. Indeed, we strongly consider the possibility that technical problems have occurred. Some studies also concluded that matrigel, being an undefined mixture of biochemicals, can cause uncertainty when interpreting data and drawing conclusions of cause and effect. Researchers have also observed biochemical inconsistencies within a single batch and between batches of matrigel (141,142). Another possible explanation for the results is the potential effects of BA and/or DMSO on the matrigel matrix, that could have affected its consistency. Due to lack of time, it was not possible to repeat the matrigel invasion experiment. However, this is an issue to be reconsidered in the future, to clarify whether, contrary to what is predicted, there may be a dual and opposite effect of BA on migration and invasion, based on distinct and still poorly understood molecular mechanisms.

6. Conclusion

The present work aimed at investigating the effects of BA on cell migration, invasion and mRNA profile of GB cells lines. The results showed that BA could hinder cell migration in the U251 cell line in a manner proportional to the treatment concentration. The mRNA profile also corroborated with these results, showing a reduction in expression of certain key genes associated with GB migration.

Downregulation of EGFR and STAT3 genes assessed in the present study seem to show that EGFR-STAT3 pathway blockade may be involved in the molecular action of BA regarding migration inhibition. These are important findings and, altogether the results allow to conclude that BA exerts antitumoral activity, being a promising compound for a novel therapeutic approach against GB. However, further research is needed to confirm the exact molecular mechanisms or signaling pathways involved in BA therapeutic action against GB.

7. References

1. Perry A, Wesseling P. Histologic classification of gliomas. Handb Clin Neurol. 2016;134:71–95.

2. Brandao M, Simon T, Critchley G, Giamas G. Astrocytes, the rising stars of the glioblastoma microenvironment. Glia. 2019 May;67(5):779–90.

3. Schaff LR, Mellinghoff IK. Glioblastoma and Other Primary Brain Malignancies in Adults: A Review. JAMA. 2023 Feb 21;329(7):574–87.

4. Weller M, Wick W, Aldape K, Brada M, Berger M, Pfister SM, et al. Glioma. Nat Rev Dis Primer. 2015 Jul 16;1(1):1–18.

5. Dn L, A P, G R, A von D, D FB, Wk C, et al. The 2016 World Health Organization Classification of Tumors of the Central Nervous System: a summary. Acta Neuropathol (Berl) [Internet]. 2016 Jun [cited 2024 Jun 19];131(6). Available from: https://pubmed.ncbi.nlm.nih.gov/27157931/

6. Kanderi T, Munakomi S, Gupta V. Glioblastoma Multiforme. In: StatPearls [Internet]. Treasure Island (FL): StatPearls Publishing; 2024 [cited 2024 Sep 12]. Available from: http://www.ncbi.nlm.nih.gov/books/NBK558954/

7. Vaz-Salgado MA, Villamayor M, Albarrán V, Alía V, Sotoca P, Chamorro J, et al. Recurrent Glioblastoma: A Review of the Treatment Options. Cancers. 2023 Aug 26;15(17):4279.

8. Zheng X, Tang Q, Ren L, Liu J, Li W, Fu W, et al. A narrative review of research progress on drug therapies for glioblastoma multiforme. Ann Transl Med. 2021 Jun;9(11):943.

9. Birzu C, French P, Caccese M, Cerretti G, Idbaih A, Zagonel V, et al. Recurrent Glioblastoma: From Molecular Landscape to New Treatment Perspectives. Cancers [Internet]. 2021 Jan [cited 2024 Jun 19];13(1). Available from: https://www.ncbi.nlm.nih.gov/pmc/articles/PMC7794906/

10. Ballabh P, Braun A, Nedergaard M. The blood-brain barrier: an overview: structure, regulation, and clinical implications. Neurobiol Dis. 2004 Jun;16(1):1–13.

11. Ou A, Yung WKA, Majd N. Molecular Mechanisms of Treatment Resistance in Glioblastoma. Int J Mol Sci [Internet]. 2021 Jan [cited 2024 Jun 19];22(1). Available from: https://www.ncbi.nlm.nih.gov/pmc/articles/PMC7794986/

12. Lau EYT, Ho NPY, Lee TKW. Cancer Stem Cells and Their Microenvironment: Biology and Therapeutic Implications. Stem Cells Int. 2017;2017:3714190.

13. Uribe D, Torres Á, Rocha JD, Niechi I, Oyarzún C, Sobrevia L, et al. Multidrug resistance in glioblastoma stem-like cells: Role of the hypoxic microenvironment and adenosine signaling. Mol Aspects Med. 2017 Jun;55:140–51.

14. Persano L, Rampazzo E, Basso G, Viola G. Glioblastoma cancer stem cells: role of the microenvironment and therapeutic targeting. Biochem Pharmacol. 2013 Mar 1;85(5):612–22.

15. Weiler M, Blaes J, Pusch S, Sahm F, Czabanka M, Luger S, et al. mTOR target NDRG1 confers MGMT-dependent resistance to alkylating chemotherapy. Proc Natl Acad Sci U S A. 2014 Jan 7;111(1):409–14.

16. Alves ALV, Gomes INF, Carloni AC, Rosa MN, da Silva LS, Evangelista AF, et al. Role of glioblastoma stem cells in cancer therapeutic resistance: a perspective on antineoplastic agents from natural sources and chemical derivatives. Stem Cell Res Ther. 2021 Mar 24;12(1):206.

17. Peppicelli S, Andreucci E, Ruzzolini J, Laurenzana A, Margheri F, Fibbi G, et al. The acidic microenvironment as a possible niche of dormant tumor cells. Cell Mol Life Sci CMLS. 2017 Mar 22;74(15):2761–71.

18. Vaupel P, Multhoff G. Accomplices of the Hypoxic Tumor Microenvironment Compromising Antitumor Immunity: Adenosine, Lactate, Acidosis, Vascular Endothelial Growth Factor, Potassium Ions, and Phosphatidylserine. Front Immunol. 2017 Dec 21;8:1887.

19. Kahlon AS, Alexander M, Kahlon A, Wright J. Lactate levels with glioblastoma multiforme. Proc Bayl Univ Med Cent. 2016 Jul;29(3):313–4.

20. Goetze K, Walenta S, Ksiazkiewicz M, Kunz-Schughart LA, Mueller-Klieser W. Lactate enhances motility of tumor cells and inhibits monocyte migration and cytokine release. Int J Oncol. 2011 Aug;39(2):453–63.

21. Hjelmeland AB, Wu Q, Heddleston JM, Choudhary GS, MacSwords J, Lathia JD, et al. Acidic stress promotes a glioma stem cell phenotype. Cell Death Differ. 2011 May;18(5):829–40.

22. Hirschhaeuser F, Sattler UGA, Mueller-Klieser W. Lactate: a metabolic key player in cancer. Cancer Res. 2011 Nov 15;71(22):6921–5.

23. Sharma A, Jasrotia S, Kumar A. Effects of Chemotherapy on the Immune System: Implications for Cancer Treatment and Patient Outcomes. Naunyn Schmiedebergs Arch Pharmacol. 2024 May;397(5):2551–66.

24. Jackson CM, Kochel CM, Nirschl CJ, Durham NM, Ruzevick J, Alme A, et al. Systemic Tolerance Mediated by Melanoma Brain Tumors is Reversible by Radiotherapy and Vaccination. Clin Cancer Res Off J Am Assoc Cancer Res. 2016 Mar 1;22(5):1161–72.

25. Topalian SL, Taube JM, Anders RA, Pardoll DM. Mechanism-driven biomarkers to guide immune checkpoint blockade in cancer therapy. Nat Rev Cancer. 2016 May;16(5):275–87.

26. Preusser M, Lim M, Hafler DA, Reardon DA, Sampson JH. Prospects of immune checkpoint modulators in the treatment of glioblastoma. Nat Rev Neurol. 2015 Sep;11(9):504–14.

27. Louveau A, Smirnov I, Keyes TJ, Eccles JD, Rouhani SJ, Peske JD, et al. Structural and functional features of central nervous system lymphatics. Nature. 2015 Jul 16;523(7560):337–41.

28. Ma R, Taphoorn MJB, Plaha P. Advances in the management of glioblastoma. J Neurol Neurosurg Psychiatry. 2021 Oct;92(10):1103–11.

29. Muir M, Gopakumar S, Traylor J, Lee S, Rao G. Glioblastoma multiforme: novel therapeutic targets. Expert Opin Ther Targets. 2020 Jul;24(7):605–14.

30. Gillet JP, Efferth T, Remacle J. Chemotherapy-induced resistance by ATP-binding cassette transporter genes. Biochim Biophys Acta. 2007 Jun;1775(2):237–62.

31. Szylberg M, Sokal P, Śledzińska P, Bebyn M, Krajewski S, Szylberg Ł, et al. MGMT Promoter Methylation as a Prognostic Factor in Primary Glioblastoma: A Single-Institution Observational Study. Biomedicines. 2022 Aug 20;10(8):2030.

32. Weller M, Stupp R, Reifenberger G, Brandes AA, van den Bent MJ, Wick W, et al. MGMT promoter methylation in malignant gliomas: ready for personalized medicine? Nat Rev Neurol. 2010 Jan;6(1):39–51.

33. Qian Z, Zhou S, Zhou Z, Yang X, Que S, Lan J, et al. miR-146b-5p suppresses glioblastoma cell resistance to temozolomide through targeting TRAF6. Oncol Rep. 2017 Nov;38(5):2941–50.

34. Makowska M, Smolarz B, Romanowicz H. microRNAs (miRNAs) in Glioblastoma Multiforme (GBM)—Recent Literature Review. Int J Mol Sci. 2023 Feb 9;24(4):3521.

35. Chen M, Medarova Z, Moore A. Role of microRNAs in glioblastoma. Oncotarget. 2021 Aug 17;12(17):1707–23.

36. Haque A, Banik NL, Ray SK. MOLECULAR ALTERATIONS IN GLIOBLASTOMA: POTENTIAL TARGETS FOR IMMUNOTHERAPY. Prog Mol Biol Transl Sci. 2011;98:187.

37. Sareen H, Ma Y, Becker TM, Roberts TL, Souza P de, Powter B. Molecular Biomarkers in Glioblastoma: A Systematic Review and Meta-Analysis. Int J Mol Sci [Internet]. 2022 Aug [cited 2024 Jun 19];23(16). Available from: https://www.ncbi.nlm.nih.gov/pmc/articles/PMC9408540/

38. Hanif F, Muzaffar K, Perveen K, Malhi SM, Simjee SU. Glioblastoma Multiforme: A Review of its Epidemiology and Pathogenesis through Clinical Presentation and Treatment. Asian Pac J Cancer Prev APJCP. 2017;18(1):3.

39. Cuddapah VA, Robel S, Watkins S, Sontheimer H. A neurocentric perspective on glioma invasion. Nat Rev Neurosci. 2014 Jul;15(7):455–65.

40. Alfonso JCL, Talkenberger K, Seifert M, Klink B, Hawkins-Daarud A, Swanson KR, et al. The biology and mathematical modelling of glioma invasion: a review. J R Soc Interface. 2017 Nov 8;14(136):20170490.

41. Nousi A, Søgaard MT, Audoin M, Jauffred L. Single-cell tracking reveals super-spreading brain cancer cells with high persistence. Biochem Biophys Rep. 2021 Dec 1;28:101120.

42. George S, Martin JAJ, Graziani V, Sanz-Moreno V. Amoeboid migration in health and disease: Immune responses versus cancer dissemination. Front Cell Dev Biol. 2023 Jan 5;10:1091801.

43. Louca M, Zaravinos A, Stylianopoulos T, Gkretsi V. ILK silencing inhibits migration and invasion of more invasive glioblastoma cells by downregulating ROCK1 and Fascin-1. Mol Cell Biochem. 2020 Aug 1;471(1):143–53.

44. Saucedo-Mora L, Sanz MÁ, Montáns FJ, Benítez JM. A simple agent-based hybrid model to simulate the biophysics of glioblastoma multiforme cells and the concomitant evolution of the oxygen field. Comput Methods Programs Biomed. 2024 Apr 1;246:108046.

45. Lau LW, Cua R, Keough MB, Haylock-Jacobs S, Yong VW. Pathophysiology of the brain extracellular matrix: a new target for remyelination. Nat Rev Neurosci. 2013 Oct;14(10):722–9.

46. Hagemann C, Anacker J, Ernestus RI, Vince GH. A complete compilation of matrix metalloproteinase expression in human malignant gliomas. World J Clin Oncol. 2012 May 5;3(5):67.

47. Velásquez C, Mansouri S, Mora C, Nassiri F, Suppiah S, Martino J, et al. Molecular and Clinical Insights into the Invasive Capacity of Glioblastoma Cells. J Oncol. 2019 Jul 29;2019:1740763.

48. Lewis-Tuffin LJ, Rodriguez F, Giannini C, Scheithauer B, Necela BM, Sarkaria JN, et al. Misregulated E-Cadherin Expression Associated with an Aggressive Brain Tumor Phenotype. PLoS ONE. 2010 Oct 27;5(10):e13665.

49. Yadati T, Houben T, Bitorina A, Shiri-Sverdlov R. The Ins and Outs of Cathepsins: Physiological Function and Role in Disease Management. Cells. 2020 Jul 13;9(7):1679.

50. Zhong S, Khalil RA. A Disintegrin and Metalloproteinase (ADAM) and ADAM with thrombospondin motifs (ADAMTS) family in vascular biology and disease. Biochem Pharmacol. 2019 Jun 1;164:188–204.

51. Mahmood N, Mihalcioiu C, Rabbani SA. Multifaceted Role of the Urokinase-Type Plasminogen Activator (uPA) and Its Receptor (uPAR): Diagnostic, Prognostic, and Therapeutic Applications. Front Oncol. 2018 Feb 12;8:24.

52. Park T, Kim B, Macapagal J, Dieriks B, Schweder P, Heppner P, et al. ANGI-03. PSA-NCAM IN GLIOBLASTOMA – A NEGATIVE PROGNOSTIC MARKER AND A THERAPEUTIC TARGET? Neuro-Oncol. 2018 Nov;20(Suppl 6):vi28–9.

53. Mahesparan R, Read TA, Lund-Johansen M, Skaftnesmo KO, Bjerkvig R, Engebraaten O. Expression of extracellular matrix components in a highly infiltrative in vivo glioma model. Acta Neuropathol (Berl). 2003 Jan;105(1):49–57.

54. Kwiatkowska A, Symons M. Signaling determinants of glioma cell invasion. Adv Exp Med Biol. 2013;986:121–41.

55. Renner G, Noulet F, Mercier MC, Choulier L, Etienne-Selloum N, Gies JP, et al. Expression/activation of α5β1 integrin is linked to the β-catenin signaling pathway to drive migration in glioma cells. Oncotarget. 2016 Aug 23;7(38):62194–207.

56. Kamino M, Kishida M, Kibe T, Ikoma K, Iijima M, Hirano H, et al. Wnt-5a signaling is correlated with infiltrative activity in human glioma by inducing cellular migration and MMP-2. Cancer Sci. 2011 Mar;102(3):540–8.

57. Kahlert UD, Maciaczyk D, Doostkam S, Orr BA, Simons B, Bogiel T, et al. Activation of canonical WNT/β-catenin signaling enhances in vitro motility of glioblastoma cells by activation of ZEB1 and other activators of epithelial-to-mesenchymal transition. Cancer Lett. 2012 Dec 1;325(1):42–53.

58. Binda E, Visioli A, Giani F, Trivieri N, Palumbo O, Restelli S, et al. Wnt5a Drives an Invasive Phenotype in Human Glioblastoma Stem-like Cells. Cancer Res. 2017 Feb 15;77(4):996–1007.

59. Hatoum A, Mohammed R, Zakieh O. The unique invasiveness of glioblastoma and possible drug targets on extracellular matrix. Cancer Manag Res. 2019 Feb 25;11:1843–55.

60. IJMS | Free Full-Text | The TGF-β Family in Glioblastoma [Internet]. [cited 2024 Sep 14]. Available from: https://www.mdpi.com/1422-0067/25/2/1067

61. Amofa KY, Patterson KM, Ortiz J, Kumar S. Dissecting TGF-β-induced glioblastoma invasion with engineered hyaluronic acid hydrogels. APL Bioeng. 2024 Jun;8(2):026125.

62. Han J, Alvarez-Breckenridge CA, Wang QE, Yu J. TGF-β signaling and its targeting for glioma treatment. Am J Cancer Res. 2015 Feb 15;5(3):945–55.

63. Fu W, Hou X, Dong L, Hou W. Roles of STAT3 in the pathogenesis and treatment of glioblastoma. Front Cell Dev Biol [Internet]. 2023 Feb 27 [cited 2024 Sep 25];11. Available from: https://www.frontiersin.org/journals/cell-and-developmental-biology/articles/10.3389/fcell.2023.1098482/full

64. Wang H, Lai Q, Wang D, Pei J, Tian B, Gao Y, et al. Hedgehog signaling regulates the development and treatment of glioblastoma. Oncol Lett. 2022 Jul 5;24(3):294.

65. Skóra B, Masicz M, Nowak P, Lachowska J, Sołtysek P, Biskup J, et al. Suppression of sonic hedgehog pathway-based proliferation in glioblastoma cells by small-size silver nanoparticles in vitro. Arch Toxicol. 2023;97(9):2385–98.

66. Schopf FH, Biebl MM, Buchner J. The HSP90 chaperone machinery. Nat Rev Mol Cell Biol. 2017 Jun;18(6):345–60.

67. Iglesia RP, Fernandes CF de L, Coelho BP, Prado MB, Melo Escobar MI, Almeida GHDR, et al. Heat Shock Proteins in Glioblastoma Biology: Where Do We Stand? Int J Mol Sci. 2019 Nov 18;20(22):5794.

68. Lou H, Li H, Zhang S, Lu H, Chen Q. A Review on Preparation of Betulinic Acid and Its Biological Activities. Molecules. 2021 Sep 14;26(18):5583.

69. Hordyjewska A, Ostapiuk A, Horecka A, Kurzepa J. Betulin and betulinic acid: triterpenoids derivatives with a powerful biological potential. Phytochem Rev. 2019 Jun 1;18(3):929–51.

70. Cunha AB, Batista R, Castro MÁ, David JM. Chemical Strategies towards the Synthesis of Betulinic Acid and Its More Potent Antiprotozoal Analogues. Molecules. 2021 Feb 18;26(4):1081.

71. De Silva D, Senarath U, Perera PK. Molecular mechanisms of antidiabetic effect of betulinic acid in lotus rhizome. Bratisl Lek Listy. 2023;124(9):707–17.

72. Jiang W, Li X, Dong S, Zhou W. Betulinic acid in the treatment of tumour diseases: Application and research progress. Biomed Pharmacother Biomedecine Pharmacother. 2021 Oct;142:111990.

73. Loe MWC, Hao E, Chen M, Li C, Lee RCH, Zhu IXY, et al. Betulinic acid exhibits antiviral effects against dengue virus infection. Antiviral Res. 2020 Dec 1;184:104954.

74. Oliveira-Costa JF, Meira CS, Neves MVG das, Dos Reis BPZC, Soares MBP. Anti-Inflammatory Activities of Betulinic Acid: A Review. Front Pharmacol. 2022 May 23;13:883857.

75. Rocha V, Quadros H, Meira C, Silva L, Carvalho D, Hodel K, et al. Potential of Triterpenic Natural Compound Betulinic Acid for Neglected Tropical Diseases New Treatments. Biomedicines. 2022 Apr 1;10(4):831.

76. Rodrigues GCS, dos Santos Maia M, de Souza TA, de Oliveira Lima E, dos Santos LECG, Silva SL, et al. Antimicrobial Potential of Betulinic Acid and Investigation of the Mechanism of Action against Nuclear and Metabolic Enzymes with Molecular Modeling. Pathogens. 2023 Mar 13;12(3):449.

77. Wang Q, Li Y, Zheng L, Huang X, Wang Y, Chen CH, et al. Novel Betulinic Acid–Nucleoside Hybrids with Potent Anti-HIV Activity. ACS Med Chem Lett. 2020 Sep 9;11(11):2290–3.

78. Chen JL, Tai YS, Tsai HY, Hsieh CY, Chen CL, Liu CJ, et al. Betulinic Acid Inhibits the Stemness of Gastric Cancer Cells by Regulating the GRP78-TGF-β1 Signaling Pathway and Macrophage Polarization. Molecules. 2023 Feb 11;28(4):1725.

79. Kim SY, Hwangbo H, Kim MY, Ji SY, Kim DH, Lee H, et al. Betulinic Acid Restricts Human Bladder Cancer Cell Proliferation In Vitro by Inducing Caspase-Dependent Cell Death and Cell Cycle Arrest, and Decreasing Metastatic Potential. Mol Basel Switz. 2021 Mar 4;26(5):1381.

80. Lee D, Lee SR, Kang KS, Ko Y, Pang C, Yamabe N, et al. Betulinic Acid Suppresses Ovarian Cancer Cell Proliferation through Induction of Apoptosis. Biomolecules. 2019 Jul 3;9(7):257.

81. Mu H, Sun Y, Yuan B, Wang Y. Betulinic acid in the treatment of breast cancer: Application and mechanism progress. Fitoterapia. 2023 Sep;169:105617.

82. Wang H, Dong F, Wang Y, Wang X, Hong D, Liu Y, et al. Betulinic acid induces apoptosis of gallbladder cancer cells via repressing SCD1. Acta Biochim Biophys Sin. 2020 Feb 3;52(2):200–6.

83. Yurasakpong L, Nantasenamat C, Nobsathian S, Chaithirayanon K, Apisawetakan S. Betulinic Acid Modulates the Expression of HSPA and Activates Apoptosis in Two Cell Lines of Human Colorectal Cancer. Mol Basel Switz. 2021 Oct 22;26(21):6377.

84. Zhao H, Mu X, Zhang X, You Q. Lung Cancer Inhibition by Betulinic Acid Nanoparticles via Adenosine 5′-Triphosphate (ATP)-Binding Cassette Transporter G1 Gene Downregulation. Med Sci Monit Int Med J Exp Clin Res. 2020 Apr 11;26:e922092-1-e922092-7.

85. Xu T, Pang Q, Wang Y, Yan X. Betulinic acid induces apoptosis by regulating PI3K/Akt signaling and mitochondrial pathways in human cervical cancer cells. Int J Mol Med. 2017 Dec;40(6):1669–78.

86. Zhai W, Ye X, Wang Y, Feng Y, Wang Y, Lin Y, et al. CREPT/RPRD1B promotes tumorigenesis through STAT3-driven gene transcription in a p300-dependent manner. Br J Cancer. 2021 Apr 12;124(8):1437–48.

87. Su D, Gao Y qiao, Dai W bo, Hu Y, Wu Y fen, Mei Q xi. Helicteric Acid, Oleanic Acid, and Betulinic Acid, Three Triterpenes from Helicteres angustifolia L., Inhibit Proliferation and Induce Apoptosis in HT-29 Colorectal Cancer Cells via Suppressing NF-κB and STAT3 Signaling. Evid-Based Complement Altern Med ECAM. 2017;2017:5180707.

88. Shin J, Lee HJ, Jung DB, Jung JH, Lee HJ, Lee EO, et al. Suppression of STAT3 and HIF-1 alpha mediates anti-angiogenic activity of betulinic acid in hypoxic PC-3 prostate cancer cells. PloS One. 2011;6(6):e21492.

89. Zeng AQ, Yu Y, Yao YQ, Yang FF, Liao M, Song LJ, et al. Betulinic acid impairs metastasis and reduces immunosuppressive cells in breast cancer models. Oncotarget. 2017 Dec 17;9(3):3794–804.

90. Sun L, Cao J, Chen K, Cheng L, Zhou C, Yan B, et al. Betulinic acid inhibits stemness and EMT of pancreatic cancer cells via activation of AMPK signaling. Int J Oncol. 2018 Oct 24;54(1):98–110.

91. Karna E, Szoka L, Palka JA. Betulinic acid inhibits the expression of hypoxia-inducible factor 1alpha and vascular endothelial growth factor in human endometrial adenocarcinoma cells. Mol Cell Biochem. 2010 Jul;340(1–2):15–20.

92. Zhang X, Hu J, Chen Y. Betulinic acid and the pharmacological effects of tumor suppression (Review). Mol Med Rep. 2016 Nov;14(5):4489–95.

93. Aswathy M, Vijayan A, Daimary UD, Girisa S, Radhakrishnan KV, Kunnumakkara AB. Betulinic acid: A natural promising anticancer drug, current situation, and future perspectives. J Biochem Mol Toxicol. 2022;36(12):e23206.

94. Liu Y, Bi Y, Mo C, Zeng T, Huang S, Gao L, et al. Betulinic acid attenuates liver fibrosis by inducing autophagy via the mitogen-activated protein kinase/extracellular signal-regulated kinase pathway. J Nat Med. 2019 Jan;73(1):179–89.

95. Ataş MN, Ertuğrul B, İplik ES, Çakmakoğlu B, Ergen A. The inhibitory effect of betulinic acid on epithelial-mesenchymal transition pathway in renal cell carcinoma. Med Oncol Northwood Lond Engl. 2022 Aug 16;39(11):170.

96. Mei L, Xu L, Wu S, Wang Y, Xu C, Wang L, et al. Discovery, structural optimization, and anti-tumor bioactivity evaluations of betulinic acid derivatives as a new type of RORγ antagonists. Eur J Med Chem. 2023 Sep 5;257:115472.

97. Huang Y, Zhu Z, Luo C, Ma C, Zhu L, Kong L, et al. Betulinic acid attenuates cognitive dysfunction, oxidative stress, and inflammation in a model of T-2 toxin-induced brain damage. Environ Sci Pollut Res Int. 2022 Jul;29(34):52098–110.

98. Abrishamdar M, Sarkaki A, Farbood Y. The effects of betulinic acid chronic administration on the motor, non-motor behaviors, and globus pallidus local field potential power in a rat model of hemiparkinsonism. Iran J Basic Med Sci. 2022 Nov;25(11):1357–63.

99. Navabi SP, Sarkaki A, Mansouri E, Badavi M, Ghadiri A, Farbood Y. The effects of betulinic acid on neurobehavioral activity, electrophysiology and histological changes in an animal model of the Alzheimer's disease. Behav Brain Res. 2018 Jan 30;337:99–106.

100. Kaundal M, Zameer S, Najmi AK, Parvez S, Akhtar M. Betulinic acid, a natural PDE inhibitor restores hippocampal cAMP/cGMP and BDNF, improve cerebral blood flow and recover memory deficits in permanent BCCAO induced vascular dementia in rats. Eur J Pharmacol. 2018 Aug 5;832:56–66.

101. Boryczka S, Bebenek E, Jastrzebska M, Kusz J, Zubko M. Crystal structure of betulinic acid–DMSO solvate. Z Für Krist. 2012 Jun 1;227(6):379–84.

102. Yuan C, Gao J, Guo J, Bai L, Marshall C, Cai Z, et al. Dimethyl sulfoxide damages mitochondrial integrity and membrane potential in cultured astrocytes. PloS One. 2014;9(9):e107447.

103. Singh M. Effect of dimethyl sulfoxide on in vitro proliferation of skin fibroblast cells. 2017 May 24;8:78–82.

104. Xu H, Zong H, Ma C, Ming X, Shang M, Li K, et al. Epidermal growth factor receptor in glioblastoma. Oncol Lett. 2017 Jul;14(1):512–6.

105. Wang H, Du X, Liu W, Zhang C, Li Y, Hou J, et al. Combination of betulinic acid and EGFR-TKIs exerts synergistic anti-tumor effects against wild-type EGFR NSCLC by inducing autophagy-related cell death via EGFR signaling pathway. Respir Res. 2024 May 20;25(1):215.

106. Chadalapaka G, Jutooru I, Burghardt R, Safe S. Drugs that target specificity proteins downregulate epidermal growth factor receptor in bladder cancer cells. Mol Cancer Res MCR. 2010 May;8(5):739–50.

107. Ciftci HI, Radwan MO, Sever B, Hamdy AK, Emirdağ S, Ulusoy NG, et al. EGFR-Targeted Pentacyclic Triterpene Analogues for Glioma Therapy. Int J Mol Sci. 2021 Oct 11;22(20):10945.

108. Li X, Wu C, Chen N, Gu H, Yen A, Cao L, et al. PI3K/Akt/mTOR signaling pathway and targeted therapy for glioblastoma. Oncotarget. 2016 Mar 7;7(22):33440–50.

109. Mao H, LeBrun DG, Yang J, Zhu VF, Li M. Deregulated Signaling Pathways in Glioblastoma Multiforme: Molecular Mechanisms and Therapeutic Targets. Cancer Invest. 2012 Jan;30(1):48–56.

110. Ou A, Ott M, Fang D, Heimberger AB. The Role and Therapeutic Targeting of JAK/STAT Signaling in Glioblastoma. Cancers. 2021 Jan 24;13(3):437.

111. El Khayari A, Bouchmaa N, Taib B, Wei Z, Zeng A, El Fatimy R. Metabolic Rewiring in Glioblastoma Cancer: EGFR, IDH and Beyond. Front Oncol. 2022 Jul 14;12:901951.

112. Li M, Wang D, He J, Chen L, Li H. Bcl-XL: A multifunctional anti-apoptotic protein. Pharmacol Res. 2020 Jan 1;151:104547.

113. Miller DM, Thomas SD, Islam A, Muench D, Sedoris K. c-Myc and Cancer Metabolism. Clin Cancer Res Off J Am Assoc Cancer Res. 2012 Oct 15;18(20):5546–53.

114. Montalto FI, De Amicis F. Cyclin D1 in Cancer: A Molecular Connection for Cell Cycle Control, Adhesion and Invasion in Tumor and Stroma. Cells. 2020 Dec 9;9(12):2648.

115. Rubiarbonone C inhibits platelet-derived growth factor-induced proliferation and migration of vascular smooth muscle cells through the focal adhesion kinase, MAPK and STAT3 Tyr705 signalling pathways - PubMed [Internet]. [cited 2024 Sep 27]. Available from: https://pubmed.ncbi.nlm.nih.gov/28832962/

116. Xue J, Zhou A, Wu Y, Morris SA, Lin K, Amin S, et al. miR-182-5p Induced by STAT3 Activation Promotes Glioma Tumorigenesis. Cancer Res. 2016 Jul 15;76(14):4293–304.

117. Meng X, Grötsch B, Luo Y, Knaup KX, Wiesener MS, Chen XX, et al. Hypoxia-inducible factor-1α is a critical transcription factor for IL-10-producing B cells in autoimmune disease. Nat Commun. 2018 Jan 17;9(1):251.

118. Masliantsev K, Pinel B, Balbous A, Guichet PO, Tachon G, Milin S, et al. Impact of STAT3 phosphorylation in glioblastoma stem cells radiosensitization and patient outcome. Oncotarget. 2017 Dec 16;9(3):3968–79.

119. Giladi ND, Ziv-Av A, Lee HK, Finniss S, Cazacu S, Xiang C, et al. RTVP-1 promotes mesenchymal transformation of glioma via a STAT-3/IL-6-dependent positive feedback loop. Oncotarget. 2015 Sep 8;6(26):22680–97.

120. Liu Q, Wang L, Wang Z, Yang Y, Tian J, Liu G, et al. GRIM-19 opposes reprogramming of glioblastoma cell metabolism via HIF1α destabilization. Carcinogenesis. 2013 Aug;34(8):1728–36.

121. Kesanakurti D, Chetty C, Rajasekhar Maddirela D, Gujrati M, Rao JS. Essential role of cooperative NF-κB and Stat3 recruitment to ICAM-1 intronic consensus elements in the regulation of radiation-induced invasion and migration in glioma. Oncogene. 2013 Oct 24;32(43):5144–55.

122. Kim BH, Lee H, Park CG, Jeong AJ, Lee SH, Noh KH, et al. STAT3 Inhibitor ODZ10117 Suppresses Glioblastoma Malignancy and Prolongs Survival in a Glioblastoma Xenograft Model. Cells. 2020 Mar 15;9(3):722.

123. Priester M, Copanaki E, Vafaizadeh V, Hensel S, Bernreuther C, Glatzel M, et al. STAT3 silencing inhibits glioma single cell infiltration and tumor growth. Neuro-Oncol. 2013 Jul;15(7):840–52.

124. Michaud-Levesque J, Bousquet-Gagnon N, Béliveau R. Quercetin abrogates IL-6/STAT3 signaling and inhibits glioblastoma cell line growth and migration. Exp Cell Res. 2012 May 1;318(8):925–35.

125. Li J, Wang X, Chen L, Zhang J, Zhang Y, Ren X, et al. TMEM158 promotes the proliferation and migration of glioma cells via STAT3 signaling in glioblastomas. Cancer Gene Ther. 2022 Aug;29(8):1117–29.

126. Zhang C, Xu H, Zhou Z, Tian Y, Cao X, Cheng G, et al. Blocking of the EGFR-STAT3 signaling pathway through afatinib treatment inhibited the intrahepatic cholangiocarcinoma. Exp Ther Med. 2018 Jun;15(6):4995–5000.

127. Jensen KV, Hao X, Aman A, Luchman HA, Weiss S. EGFR blockade in GBM brain tumor stem cells synergizes with JAK2/STAT3 pathway inhibition to abrogate compensatory mechanisms in vitro and in vivo. Neuro-Oncol Adv. 2020 Feb 18;2(1):vdaa020.

128. Long L, Fei X, Chen L, Yao L, Lei X. Potential therapeutic targets of the JAK2/STAT3 signaling pathway in triple-negative breast cancer. Front Oncol [Internet]. 2024 Apr 18 [cited 2024 Sep 29];14. Available from: https://www.frontiersin.org/journals/oncology/articles/10.3389/fonc.2024.1381251/full

129. Loh CY, Chai JY, Tang TF, Wong WF, Sethi G, Shanmugam MK, et al. The E-Cadherin and N-Cadherin Switch in Epithelial-to-Mesenchymal Transition: Signaling, Therapeutic Implications, and Challenges. Cells. 2019 Sep 20;8(10):1118.

130. Rubtsova SN, Zhitnyak IY, Gloushankova NA. Dual role of E-cadherin in cancer cells. Tissue Barriers. 10(4):2005420.

131. Farooqi AA, Turgambayeva A, Tashenova G, Tulebayeva A, Bazarbayeva A, Kapanova G, et al. Multifunctional Roles of Betulinic Acid in Cancer Chemoprevention: Spotlight on JAK/STAT, VEGF, EGF/EGFR, TRAIL/TRAIL-R, AKT/mTOR and Non-Coding RNAs in the Inhibition of Carcinogenesis and Metastasis. Molecules. 2022 Dec 21;28(1):67.

132. He D, Chen Y, Zhou Y, Zhang S, Hong M, Yu X, et al. Phytochemical library screening reveals betulinic acid as a novel Skp2-SCF E3 ligase inhibitor in non–small cell lung cancer. Cancer Sci. 2021 Aug;112(8):3218–32.

133. Chintharlapalli S, Papineni S, Ramaiah SK, Safe S. Betulinic acid inhibits prostate cancer growth through inhibition of specificity protein transcription factors. Cancer Res. 2007 Mar 15;67(6):2816–23.

134. Gao Y, Jia Z, Kong X, Li Q, Chang DZ, Wei D, et al. Combining betulinic acid and mithramycin A effectively suppresses pancreatic cancer by inhibiting proliferation, invasion and angiogenesis. Cancer Res. 2011 Aug 1;71(15):5182–93.

135. Pandey MK, Sung B, Aggarwal BB. Betulinic Acid Suppresses STAT3 Activation Pathway Through Induction of Protein Tyrosine Phosphatase SHP-1 in Human Multiple Myeloma Cells. Int J Cancer J Int Cancer. 2010 Jul 15;127(2):282–92.

136. Jj Y, Yj L, Js K, Dg K, Hs L. Betulinic acid inhibits high glucose-induced vascular smooth muscle cells proliferation and migration. J Cell Biochem [Internet]. 2010 Dec 15 [cited 2024 Sep 27];111(6). Available from: https://pubmed.ncbi.nlm.nih.gov/20872792/

137. Zheng Y, Liu P, Wang N, Wang S, Yang B, Li M, et al. Betulinic Acid Suppresses Breast Cancer Metastasis by Targeting GRP78-Mediated Glycolysis and ER Stress Apoptotic Pathway. Oxid Med Cell Longev. 2019 Aug 19;2019:8781690.

138. Yoon JJ, Lee YJ, Kang DG, Kim JS, Lee HS. Inhibitory effect of betulinic acid on TNF-α-induced adhesion molecule and its related signaling. FASEB J. 2009;23(S1):937.10-937.10.

139. Li N, Gong Z, Li X, Ma Q, Wu M, Liu D, et al. Betulinic acid inhibits the migration and invasion of fibroblast-like synoviocytes from patients with rheumatoid arthritis. Int Immunopharmacol. 2019 Feb 1;67:186–93.

140. Liao L, Liu C, Xie X, Zhou J. Betulinic acid induces apoptosis and impairs migration and invasion in a mouse model of ovarian cancer. J Food Biochem. 2020;44(7):e13278.

141. Wright C, Widdowson J. Alternatives to scarce Matrigel and why they are needed. 2022 Jun 1;

142. Benton G, Kleinman HK, George J, Arnaoutova I. Multiple uses of basement membrane-like matrix (BME/Matrigel) in vitro and in vivo with cancer cells. Int J Cancer. 2011 Apr 15;128(8):1751–7.